

Training and Communication for
Earthquake Risk Assessment
TREQ Project

Seismic Hazard Results (rock and soil conditions)

Deliverable 2.2.3 – Version 2.0.0



**Global
Earthquake
Model (GEM)
Foundation**

www.globalquakemodel.org

Description of the hazard results on rock
and soil for the three cities in the urban
hazard assessment component of TREQ

Seismic Hazard Results (rock and soil conditions)

Deliverable D2.2.3

Technical report produced in the context of the TREQ project

Version 2.0.0 – October, 2021

J. Garcia², K. Johnson¹

¹Global Earthquake Model Foundation

²Formerly Global Earthquake Model Foundation

Collaborators

The authors would like to thank the Municipal offices of the cities of Quito, Cali and Santiago de los Caballeros, for their invaluable contribution to the project, including but not limited to collecting local data, organizing meetings and communicating the results to stakeholders and the general public.

The authors would also like to thank the partners for their support:

- Servicio Geológico Colombiano (SGC)
- Servicio Geológico Nacional (SGN) de la República Dominicana
- El Instituto Geofísico de la Escuela Politécnica Nacional (IG-EPN)

Acknowledgements

This report forms part of the United States Agency for International Development (USAID) and the Bureau of Humanitarian Assistance (BHA) funded program for Training and Communication for Earthquake Risk Assessment (TREQ) project, grant AID-OFDA-G-720FDA19GR00273. The Global Earthquake Model Foundation manage and executes the resources of USAID and implements the project in collaboration with local stakeholders.

The TREQ Project is designed to demonstrate how earthquake hazard and risk assessment can inform decision makers in the development of risk reduction policies, as well as how earthquake risk can be properly communicated to stakeholders and the public in general. Specifically, the project aims to develop capacity for urban earthquake risk assessment in Latin America, Quito (Ecuador), Cali (Colombia), and Santiago de los Caballeros (Dominican Republic), while the second part will produce training, educational and communication materials that will enhance the understanding of earthquake risk worldwide. This program targets a wide spectrum of stakeholders, categorized into four main groups: governance (decision-makers/public authorities), industry (practitioners and professionals), academia (researchers and professors), and the community.

This report has been made possible thanks to the support and generosity of the American people through the United States Agency for International Development (USAID) and the Bureau of Humanitarian Assistance (BHA). The opinions, findings, and conclusions stated herein are those of the authors and do not necessarily reflect the views of USAID or the United States Government.

Citation: Garcia J., Johnson K. (2021) Seismic Hazard Results (rock and soil conditions). GEM-TREQ project technical report, deliverable D.2.2.3, v2.0.0, October 2021.

License

Except where otherwise noted this work is made available under the terms of Creative Commons License Attribution - ShareAlike 4.0 International (CC BY-NC-SA 4.0). You can download this report and share it with others as long as you provide proper credit, but you cannot change it in any way or use it commercially.

The views and interpretations in this document are those of the individual author(s) and should not be attributed to the GEM Foundation. With them also lies the responsibility for the scientific and technical data presented. The authors have taken great care to ensure the accuracy of the information in this report, but accept no responsibility for the material, nor do they accept responsibility for any loss, including consequential loss incurred from the use of the material.

Copyright © 2021 GEM Foundation.

<http://www.globalquakemodel.org/>

Table of contents

	Page
1 Introduction	4
2 Santiago de Cali, Colombia	5
2.1 Reference National Seismic Hazard Model (NSHM)	5
2.2 Seismic hazard results on Rock.....	12
2.2.1 Hazard results on reference bed rock.....	12
2.3 Seismic hazard results on Soil	14
2.3.1 Results using Vs30 from USGS.....	16
2.4 Comparison of results and discussion.....	16
3 San Francisco de Quito, Ecuador	18
3.1 Reference National Seismic Hazard Model (NSHM)	18
3.2 Seismic hazard results on Rock.....	21
3.2.1 Hazard results on reference bed rock.....	21
3.3 Seismic hazard results on Soil	23
3.3.1 Results using Vs30 from USGS.....	23
3.4 Comparison of results and discussion.....	24
4 Santiago de los Caballeros, The Dominican Republic.....	25
4.1 Reference NSHM	25
4.2 Seismic hazard results on Rock.....	26
4.3 Seismic hazard results on Soil	26
4.3.1 Results using Vs30 from USGS.....	27
5 Conclusions	27
6 References	29

1 Introduction

Assessing earthquake shaking hazard at an urban scale is the major goal of the seismic hazard component of TREQ. Detailed urban seismic hazard results must be built for the selected cities including the effects of local geology, together with soils, which usually are not incorporated into regional seismic hazard results (Figure 1).

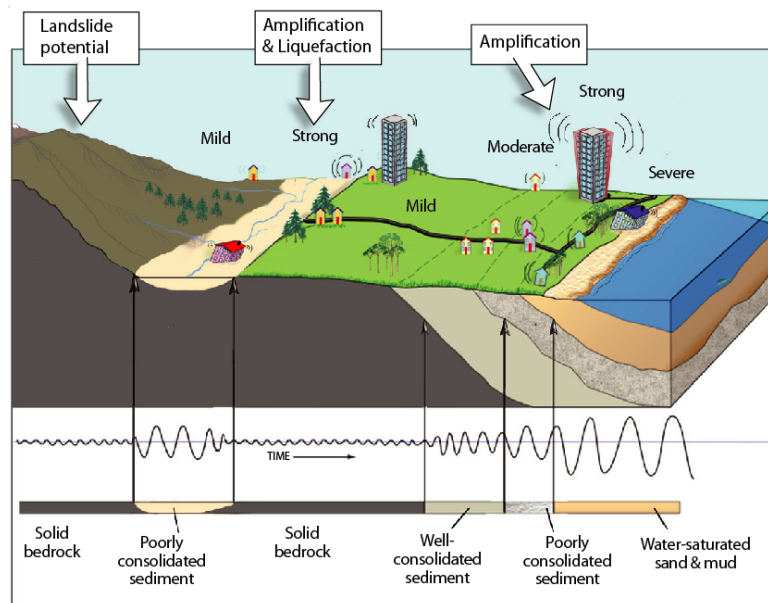


Figure 1. Earthquake effects at an urban scale. Source : <https://serc.carleton.edu/205923>

The first task was a critical review of the available PSHA models for the selected cities and the selection of a reference PSHA/NSHM model to be used for rock and soil calculations (see more details in D2.2.1 and D2.2.2 reports). The selected national seismic hazard models (NSHM) have been used to compute seismic hazard on reference bedrock, as well as on soil condition using a simplified approach, which accounts for expected ground shaking on soil using the time-averaged velocity of shear waves in the uppermost 30 m of the subsurface (V_{s30}). The V_{s30} velocity is part of the site-term in the modern ground motion prediction equations (GMPEs) used in PSHA/NSHM. For these simplified soil calculations, the V_{s30} global model proposed by the USGS (Allen and Wald, 2007) were used to create a site-model for each city following the OpenQuake standards. In the following sections for each city, we describe the main characteristic of the reference PSHA model used, and the results computed for rock and soil conditions for grid covering the city.

The hazard calculations were performed for rock and soil conditions using the OpenQuake Engine (Pagani et al. 2014), on a grid covering the city (1km spaced) and for 10% and 2% in 50 years probabilities of exceedance (PoE). Several structural periods (i.e. peak ground acceleration and spectral acceleration at 0.2, 0.5, 1.0 and 2.0 seconds) were considered. Uniform hazard spectra (UHS) were derived using these spectral periods for the PoE considered. In addition, disaggregation analysis was performed for each city in order to understand which sources contribute most to the hazard computed for rock condition for each city.

2 Santiago de Cali, Colombia

2.1 Reference National Seismic Hazard Model (NSHM)

For Santiago de Cali, Colombia, the NSHM model proposed by Arcila et al. (2020) was selected as reference PSHA model. The NSHM was created in the framework of a three-year scientific collaboration between the Servicio Geológico Colombiano (SGC) and the GEM Foundation. To build the model, a new homogeneous earthquake catalogue was compiled by SGC, using revised historical information and instrumental data for global (ISC, ISC-GEM, GCMT) and regional/local sources. In addition, a multidisciplinary approach (see details in Arcila et al., 2017, 2020) improved the current knowledge about active tectonic and crustal deformation in the Colombian territories, giving the possibility to develop a complex seismic source characterization (SSC). The new state-of-the-knowledge was used to pre-process the earthquake catalogue and obtain specific sub-catalogues of main events (mainshocks) for each of the tectonic environment considered. The tectonic classification of the events into the main tectonic contexts is crucial to developing a SSC in a complex seismotectonic environment like Colombia. Details about the classification can be found in Arcila et al. (2020). For each sub-catalogue the typical pre-processing analysis was performed (i.e., catalogue declustering and filtering for completeness).

The SSC was divided into four components, which account for the different seismotectonic environment identified in the study region. An active shallow source model, containing 30 independent area sources (see Table 1), defined using the classical approach (i.e. regions with homogeneous temporal and spatial characteristic of seismicity, tectonic and geodynamic setting) were used. A summary of main parameters characterizing these sources is presented In Table 1.

Table 1. Main parameters characterizing seismicity of the area sources of the crustal model. In bold the sources mainly affecting Santiago de Cali city. Id: code identifying the seismic source. Name: name identifying the seismic source. a, b: parameters of the magnitude frequency distribution. Mmin, Mmax: minimum and maximum magnitude (Mw) considered. Usd, Lsd: Upper and Lower depths (km) limiting the ruptures produced by the source.

Id	Name	a	b	Mmin	Mmax	Usd	Lsd
cc01	Oriente Panamá	3.82	1.00	5.0	7.2	0	40
cc02	Pacífico Norte (Darién)	4.62	1.00	5.0	7.4	0	40
cc03	Sábanas costeñas	3.61	0.94	5.0	6.8	0	40
cc04	Ciénagas del Caribe	3.45	0.83	5.0	6.5	0	40
cc05	Perijá - Sierra Nevada	3.48	0.92	5.0	6.5	0	40
cc06	Depresión de Maracaibo	1.59	0.43	5.0	6.5	0	40
cc07	Andes de Mérida	4.15	0.90	5.0	7.9	0	40
cc08	Transversal del Caribe (Oca)	2.75	0.80	5.0	6.7	0	40
cc09	Transversal de Falcón	3.12	0.79	5.0	6.7	0	40
cc10	Guajira - Paraguaná	4.78	1.10	5.0	6.7	0	40
cc11	Pacífico Central	4.23	1.02	5.0	6.5	0	40
cc12	Norte Cordillera Central	3.66	0.92	5.0	6.5	0	40
cc13	Magdalena Medio	3.35	0.78	5.0	6.5	0	40
cc14	Norte Santander	4.18	1.06	5.0	6.5	0	40
cc15	Cocuy	3.72	0.86	5.0	7.5	0	40
cc16	Pacífico Sur	2.82	0.74	5.0	6.8	0	40
cc17	Cauca - Patía	2.05	0.61	5.0	6.8	0	40
cc18	Central Cordillera Central	2.55	0.70	5.0	7.1	0	40

cc19	Valle Alto del Magdalena	3.65	1.09	5.0	6.5	0	40
cc20	Altiplano Cundiboyacense	3.14	0.83	5.0	6.8	0	40
cc21	Piedemonte Orinoquía	4.16	0.97	5.0	6.8	0	40
cc22	Zona Andina Nariñense	2.63	0.69	5.0	7.0	0	40
cc23	Sur Cordillera Oriental	4.75	1.17	5.0	7.0	0	40
cc24	Piedemonte Amazonía	3.76	1.03	5.0	7.4	0	40
cc25	Craton	3.55	0.93	5.0	6.6	0	40
cc26	Pacífico Ecuatoriano	5.13	1.27	5.0	7.5	0	40
cc27	Sierra occidental ecuatoriana	5.66	1.34	5.0	7.6	0	40
cc28	Sierra oriental ecuatoriana	5.22	1.22	5.0	7.4	0	40
cc29	Piedemonte ecuatoriano	4.91	1.23	5.0	6.7	0	40
cc30	Zona insular de San Andrés	1.74	0.54	5.0	6.5	0	40

The second component, also for active shallow environment, was created by integrating active faults and point sources (Figure 2b). To model distributed seismicity, we grouped the shallow seismicity compiled in the catalogue into 10 wide area sources and computed a representative magnitude frequency distribution (MFD) following the same approach of the previous model. Then, the MFD was distributed across a mesh of equally spaced point sources covering the area, transforming the area source into a grid of point sources representing in a discrete form the seismicity within the source. The distribution of the seismicity rates was done using a smoothing approach, similar to Frankel (1995), which creates for each point source an MFD where rates are "smoothed" using a Gaussian kernel. The major characteristics of the wide area sources used to build the distribution seismicity model are listed in Table 2.

Table 2. Main parameters characterizing seismicity of the distributed seismicity crustal model. In bold the sources mainly affecting Santiago de Cali city. Id: code identifying the seismic source. Name: name identifying the seismic source. a, b: parameters of the magnitude frequency distribution. Mmin, Mmax: minimum and maximum magnitude (M_w) considered. Usd, Lsd: Upper and Lower depths (in km) limiting the ruptures produced by the source

Id	Name	a	b	Mmin	Mmax	Usd	Lsd
p00	Panamá	4.06	1.03	5.0	7.2	0	35
c00	Guajira - Paraguaná	3.99	0.93	5.0	6.7	0	35
c01	Pacífica	4.98	1.06	5.0	7.4	0	35
c02	Nororiental	4.20	0.97	5.0	6.5	0	35
c03	Piedemonte oriental	4.52	0.92	5.0	7.9	0	35
c04	Oca - Falcon	3.45	0.85	5.0	6.7	0	35
c05	Andina	4.48	0.96	5.0	7.1	0	35
c06	Caribe	4.45	1.05	5.0	6.8	0	35
c07	Cratón	4.63	1.16	5.0	6.6	0	35
c08	Insular San Andres	1.74	0.54	5.0	6.5	0	40

The active shallow fault sources were modelled using the Fault Modeller tool of the OpenQuake Model Building Toolkit (<https://github.com/GEMScienceTools/oq-mbtk>). In this case, the fault sources were built using tectonic estimates (geometry of the faults, area of maximum rupture, slip rate) rather than seismicity compiled in the catalogue. The MFDs characterizing the fault sources were computed following some premises: 1) the MFD follows a doubled-truncated Gutenberg-Richter distribution, 2) the minimum magnitude was arbitrarily assumed as M_w 6.5, 3) the maximum magnitude bounding the MFD depends on the fault's area (M_{max} implies a full-fault rupture) and was computed using Leonard (2010) scaling relation, 4) the b-value is assumed to be equal to those obtained for the area enclosing the fault (i.e. wide distributed

seismicity zones of Table 2) and 5) the total moment release rate is taken as the product of the slip-rate, the fault-plane area, and the aseismic coefficient. Overall, the fault model consists of 171 active fault sources spatially distributed across the Colombian territories (see Figure 2b).

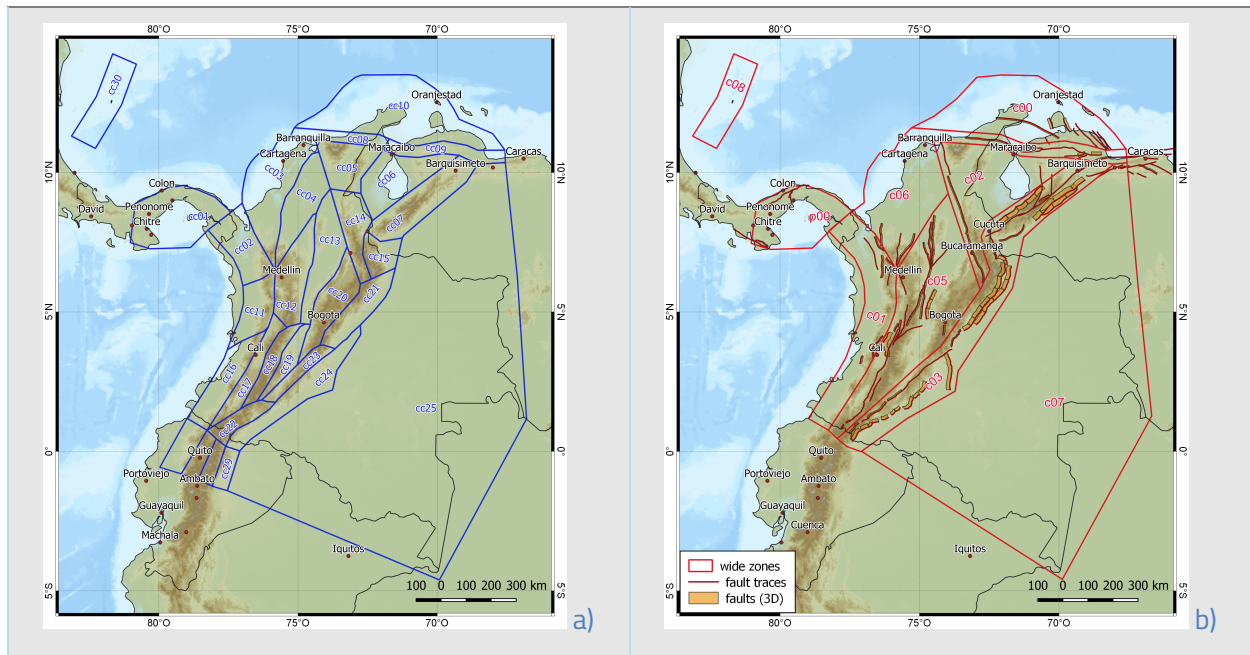


Figure 2. Shallow crustal models for Colombia 2018 PSHA study: a) area source classical model and b) distributed seismicity model (wide zones) + active fault sources. Source: Arcila et al. (2020)

To avoid double counting of seismicity, in areas where there is overlap with the surface projection of a fault source (including a buffer of 15 km around it), the MFDs of the distributed seismicity point sources were truncated at $M_{\max} = 6.5$, which was the fault source M_{\min} value considered to compute the MFD of the faults.

The third model characterizes the seismic sources related with the Nazca subduction in the western part of the country. Large "complex" faults were used to model the interface sources, while a set of non-parametric ruptures dipping at 45° and 135° and constrained by the upper and lower limits of the slab characterizes the intra-slab seismicity. Two alternative subduction models were considered (i.e. segmented and unsegmented). These models are presented in Figure 3 and Figure 4a.

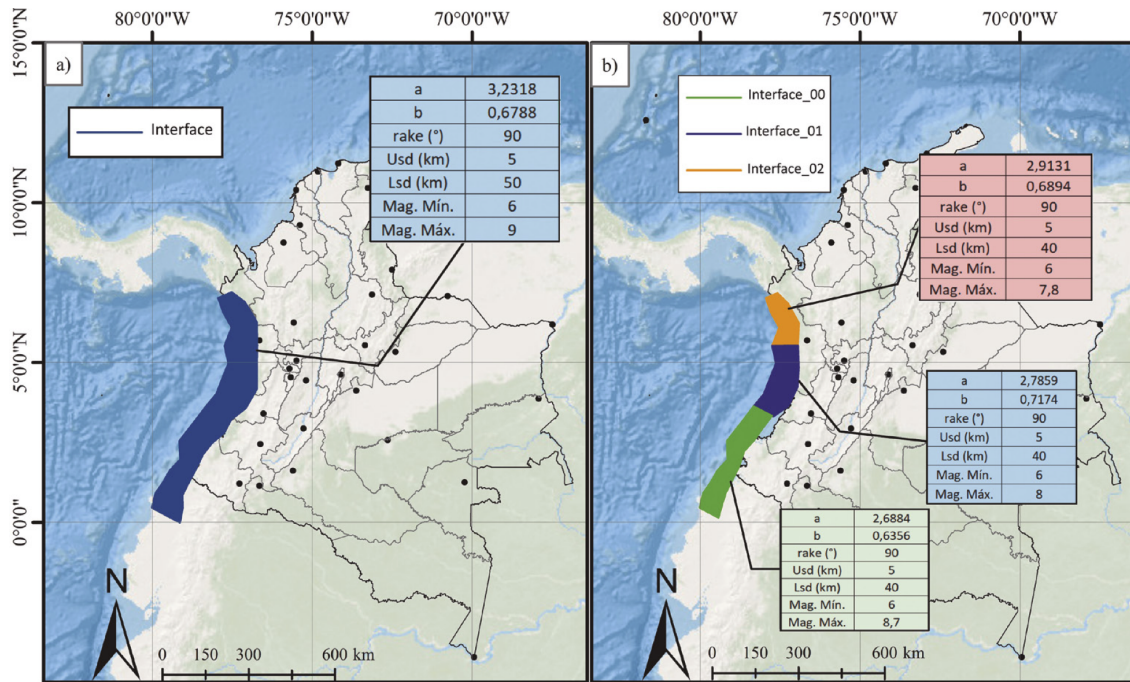


Figure 3. Subduction interface models for Colombia 2018 PSHA study: a) un-segmented model and b) segmented model. The main characteristics of the sources are presented in the tables. Source: Arcila et al. (2020).

The last component characterizes the Bucaramanga Nest, a unique Colombian tectonic environment of deep seismicity not related with the Nazca subduction. A set of non-parametric ruptures (Figure 4b) divided into two segments were used to characterize the sources related to this tectonic environment.

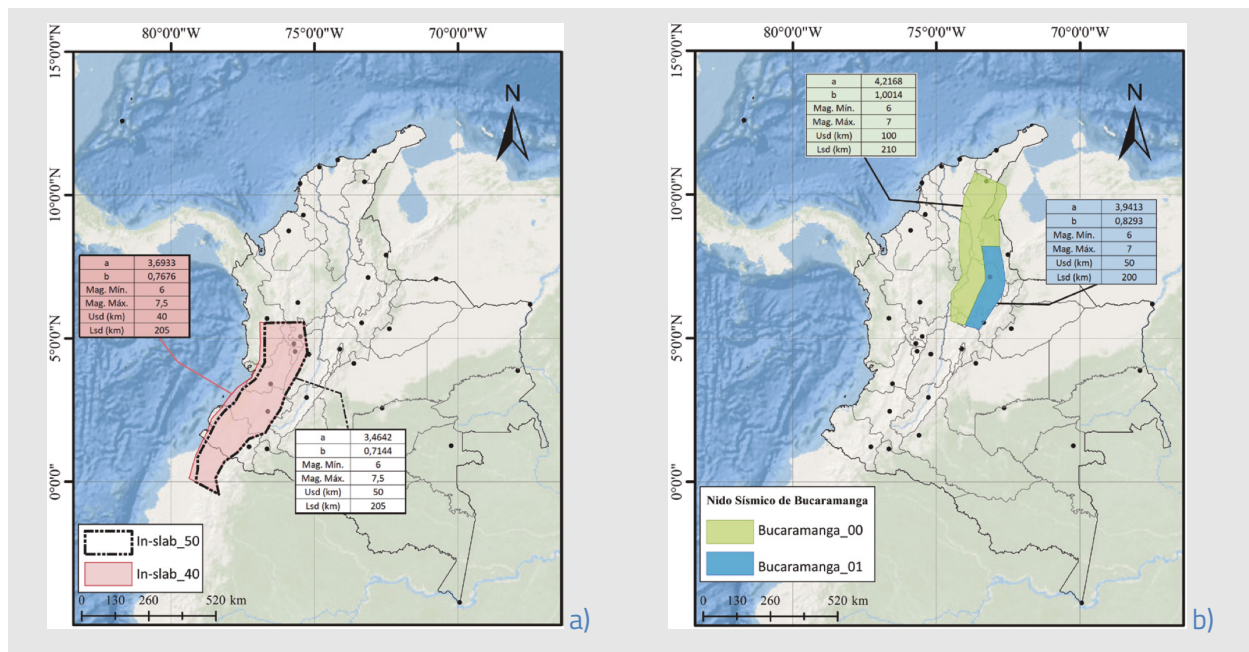


Figure 4. Seismic hazard models for Colombia 2018 PSHA study: a) In-slab models and b) Deep seismicity model. The main characteristics of the sources are presented in the tables. Source: Arcila et al. (2020).

The ground motion characterization (GMC) of this NSHM benefits from the strong-motion recordings collected by the SGC in the last decades. These data were used to perform an accurate selection of the most appropriate GMPEs for each tectonic environment (see Table 3). The selection process follows the classical procedure: a) pre-selection of candidate GMPEs, b) comparison of predicted ground shaking using trellis plots and c) data-to-predicted ground motion comparison using observed ground motion (from recordings) and those predicted by the pre-selected GMPEs. More details about the selection procedure can be found in Arcila et al. (2020).

Table 3. Ground motion models (and weights) per tectonic environment for Colombia. Source: Arcila et al., (2020).

Active Shallow Crust	
Idriss2014	0.399
CauzziEtAl2014	0.390 0.600
AbrahamsonEtAl2014	0.211 0.400

Subduction Interface	
AbrahamsonEtAl2015SInter	0.437
ZhaoEtAl2006SInterNSHMP2008	0.348
MontalvaEtAl2017SInter	0.215

Subduction IntraSlab	
MontalvaEtAl2017SSlab	0.437
AbrahamsonEtAl2015SSlab	0.358
ZhaoEtAl2006SSlabNSHMP2014	0.205

Deep Seismicity	
ZhaoEtAl2006SSlabNSHMP2014	0.443
AbrahamsonEtAl2015SSlab	0.285
MontalvaEtAl2017SSlab	0.272

In the PSHA model proposed by Arcila et al. (2020) for Colombia, epistemic uncertainties related with both, SSC and GMC were considered. Arcila et al. (2020) computed hazard using the OpenQuake engine. Hazard curves, maps and UHS for several return periods (i.e. 31, 225, 475, 975 and 2475 years) were obtained in a regular grid (~ 10 km spacing) covering the Colombian territories. The reference soil condition was a soil with V_{s30} of 760 m/s for several intensity measures (PGA and spectral acceleration at 0.1, 0.2, 0.3, 0.5, 0.7, 1.0, 1.5, 2.0, 2.5, 3.0, 4.0 and 5.0 seconds).

As an example, the hazard map for PGA with a return period of 2475 years, which corresponds to a 2% probability of exceedance in 50 years, is presented in Figure 5. As expected, the highest hazard values are distributed along the pacific coast, where the hazard is dominated by the contribution of subduction sources. The impact of some shallow active faults is also evident (i.e. Cucutá region). In Santiago de Cali, the hazard reaches ~ 0.68g for PGA and larger than 1.75g for SA at 0.2 seconds for 2% PoE in 50 years. This

confirms that Santiago de Cali is one of the most exposed cities of Colombia and for sure the most exposed between the larger and economically important Colombian cities.

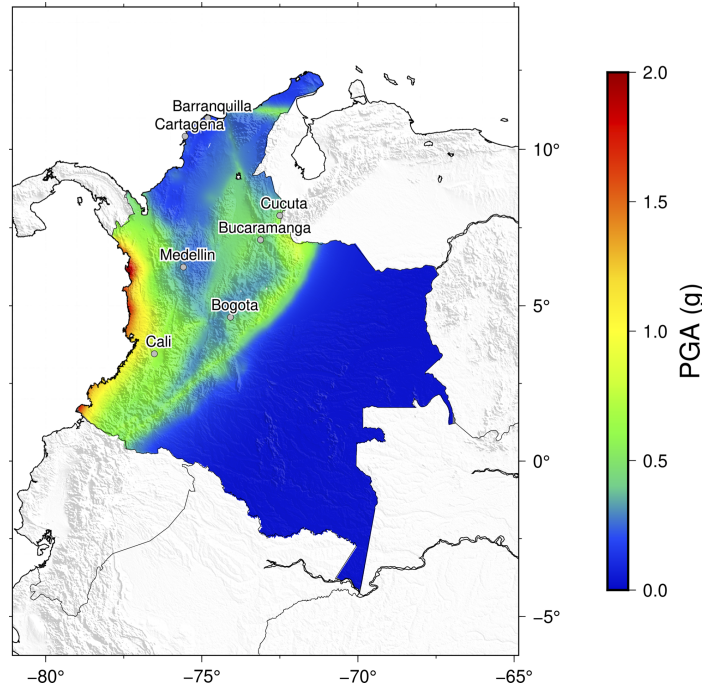


Figure 5. Mean PGA with 2% PoE in 50 years for Colombia from Arcila et al. (2020). The reference soil condition is rock ($V_{s30} = 760$ m/s).

Considering the geographic location of the Santiago de Cali city, it is expected to be most affected by the nearest crustal earthquakes, as well as by interface and intraslab events from the Nazca subduction. This is confirmed by the disaggregation analysis (Bazzurro and Cornell, 1999) performed for this city by Arcila et al. (2020). In Figure 6 the contributions to the hazard computed for the city by a combination of magnitude and distance (Figure 6a) and the tectonic environment considered (Figure 6b) are presented.

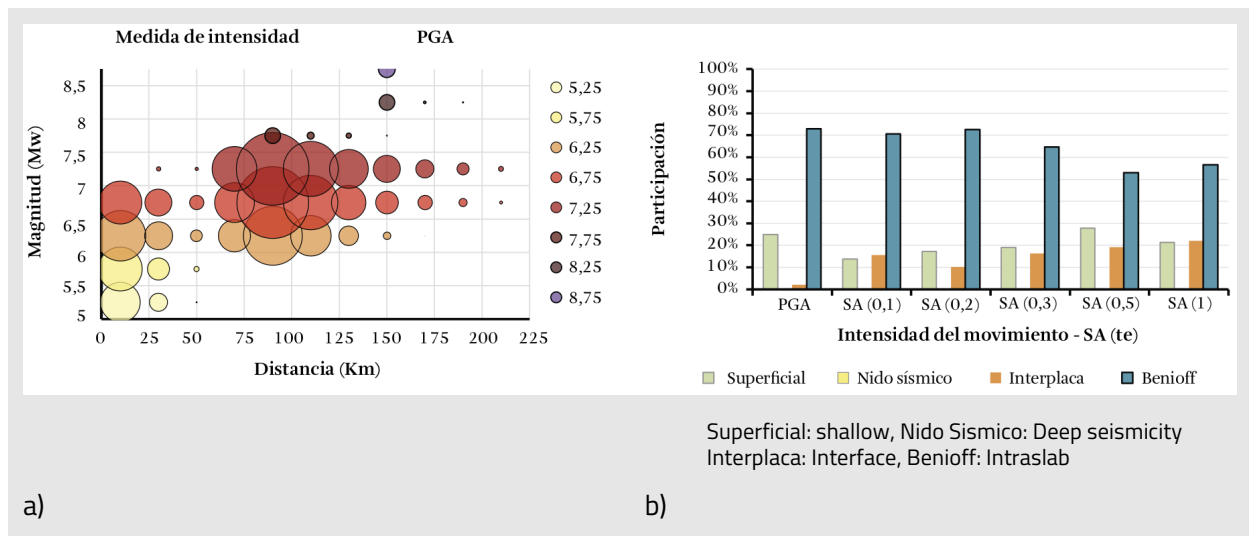


Figure 6. Disaggregation results for Santiago de Cali city: a) mean PGA with a 10% PoE in 50 years and a combination of magnitude and distance and b) disaggregation by TRT for different intensities measure types.

Source: Arcila et al. (2020).

From Figure 6a it is evident that sources at two different distances can affect the city. The first distance is close to the city (within 25 km) with $M_w \sim 5.5 - 7.0$. This cluster should be related to active shallow faulting nearest to the city, since subduction sources are more distant. A second cluster at $\sim 80 - 100$ km distance, with larger magnitudes (and contribution) is also present. The disaggregation results in Figure 6b, confirm these points and add new valuable information: the subduction sources that contribute most are the intraslab ones. Figure 6b also shows that Santiago de Cali city is not affected by the deep seismicity sources.

To compute hazard calculations for Santiago de Cali using the Arcila et al. (2020) model, one modification was needed. Since in this model only faults with recognized tectonic activity were considered, the Cauca-Cali-Patia fault, classified as potentially active into the Colombian Geological Survey Database of active faults, was excluded a priori. However, this fault was modelled by the authors of the microzonation study of the city (INGEOMINAS-DAGMA, 2005) and in the last two hazard studies used as a reference for the Colombian building codes (AIS, 2019; Salgado et al. 2016; Bernal, 2014). Due the vicinity of the fault to the study region, in all these studies its contribution to the total hazard is significant (see Figure 7) and, as a consequence, we decided to implement the Cauca-Cali-Patia fault as an active fault source during this study.

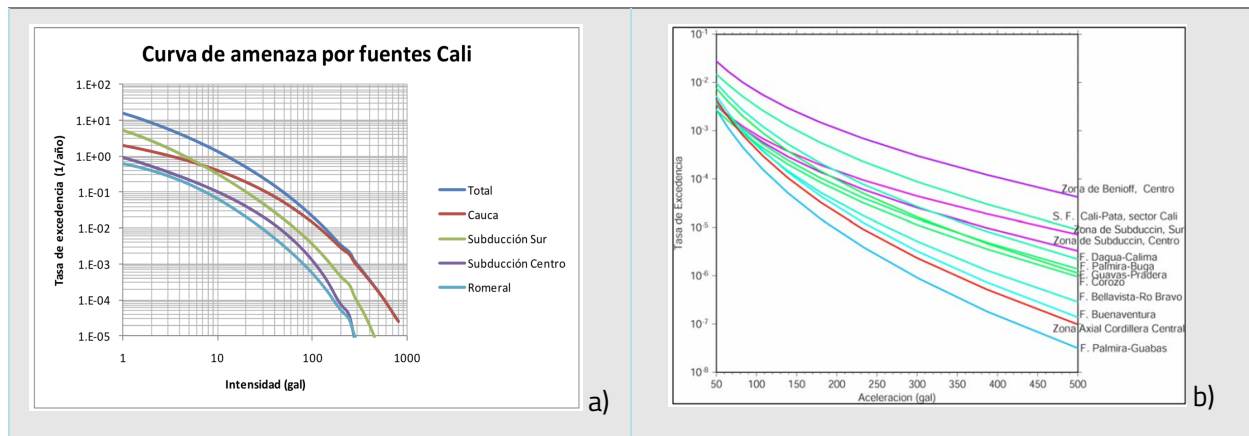


Figure 7. Contribution by sources to PGA for Santiago de Cali city: a) AIS (2019) and b) INGEOMINAS-DAGMA (2005).

The implementation follows the same methodology used in Arcila et al. (2020), the parameters related with the geometry of the fault (i.e. fault trace, style-of-faulting, segmentation) were obtained from the database of active fault of the SGC. The fault kinematics and slip rate estimates were based on a recent study about the stress and strain regime in Colombia using earthquake focal mechanisms and geodetic data by Arcila and Muñoz–Martín (2020). In Figure 8 the fault trace is presented, and in Table 4 the main parameters are listed.

Table 4. Main configuration parameters used to implement the Cauca-Cali-Patia fault. The Dip value units are degrees, and the slip-rate value one in mm/year.

Fault(segment)	Dip	Dip_dir	Slip_type	Slip_rate
Cauca-Cali-Patia 01	85	West	Dextral	0.1

Cauca-Cali-Patia 02	85	West	Dextral	0.1
Cauca-Cali-Patia 03	85	West	Dextral	0.1
Cauca-Cali-Patia 04	85	West	Dextral	0.1
Cauca-Cali-Patia 05	85	West	Dextral	0.2
Cauca-Cali-Patia 06	85	West	Dextral	0.2

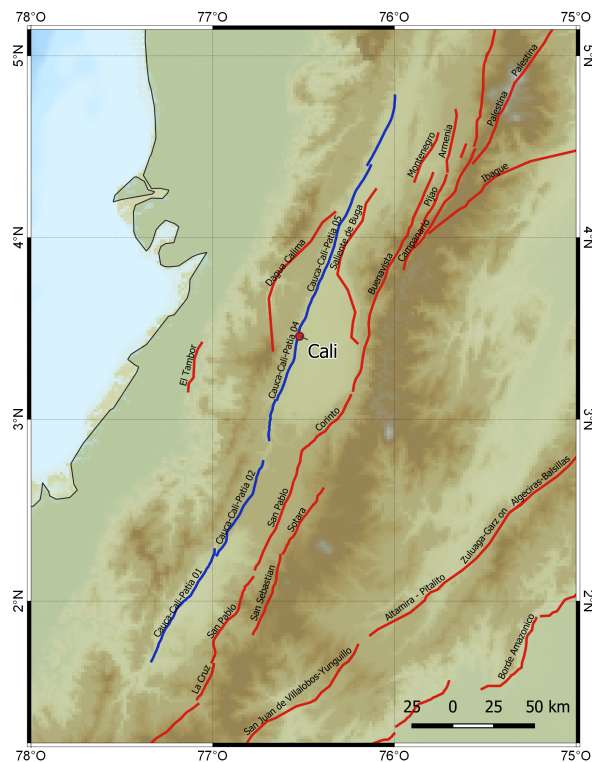


Figure 8. Faults in the Cauca Valley region. The blue lines are the traces of the Cauca-Cali-Patia fault (segments) and in red those considered by Arcila et al. (2020).

2.2 Seismic hazard results on Rock

2.2.1 Hazard results on reference bed rock

In seismology and earthquake engineering studies, two types of bedrocks are used. In seismology/geophysics the "seismic bedrock" is used to define an interface with a shear wave velocity of ~ 3000 m/s, usually located within the upper crust. In contrast, the earthquake engineer prefers to use a shallower interface, which the underlying stratum has a shear wave velocity from 300 – 1000 m/s. This interface is called "engineering bedrock" and it is mostly defined as 760 – 800 m/s in ground motion prediction and simulation studies.

In the microzonation study of Santiago de Cali (INGEOMINAS-DAGMA, 2005), geophysical investigations performed in the city provided important information about the contact between the tertiary rock and the bedrock (see Figure 21 in D2.2.1). The depth of the bedrock increases toward the east, with maximum values of 2.6 km in the Navarro sector and 2.3 km in the northern part of the city. On the west side, the depth of the bedrock decreases and the average thickness of the sediments is ~ 1.0 km.

Also, seismic refraction lines were performed and used to identify the propagation velocity of the longitudinal (V_p) and transversal (V_s) waves in the city. The thickness of the sedimentary deposits and the depth of the bedrock obtained using seismic refraction techniques are consistent with those obtained by other methods (i.e. gravity campaign), but the V_p and V_s velocities are larger than those expected for similar lithological and geological units in other regions (see details in INGEOMINAS-DAGMA, 2005, Informe 3). The V_s values range between 700 – 1600 m/s in the interface between the sedimentary not consolidated deposits and deeper sedimentary deposits or tertiary rocks. For the hazard calculation on a reference bedrock we considered that a $V_s = 800$ m/s could be a good compromise.

The hazard calculations were performed for a grid covering the city (1 km spaced). Hazard maps, curves and UHSs were obtained for intensity measures PGA, SA at periods of 0.2 and 1.0 sec with 10% and 2% PoE in 50 years and for a reference bedrock equivalent to $V_{s30} = 800$ m/s.

In Figure 9, the PGA maps for rock conditions are presented. In both cases, the highest PGA values are located at the west side of the city, reaching 0.38g and 0.70g for 10% and 2% PoE in 50 years, respectively. The hazard values decreasing for the central and eastern part of the city, with values mostly range 0.35 – 0.37g for 10% PoE in 50 years and 0.66 – 0.70g for 2% PoE in 50 years.

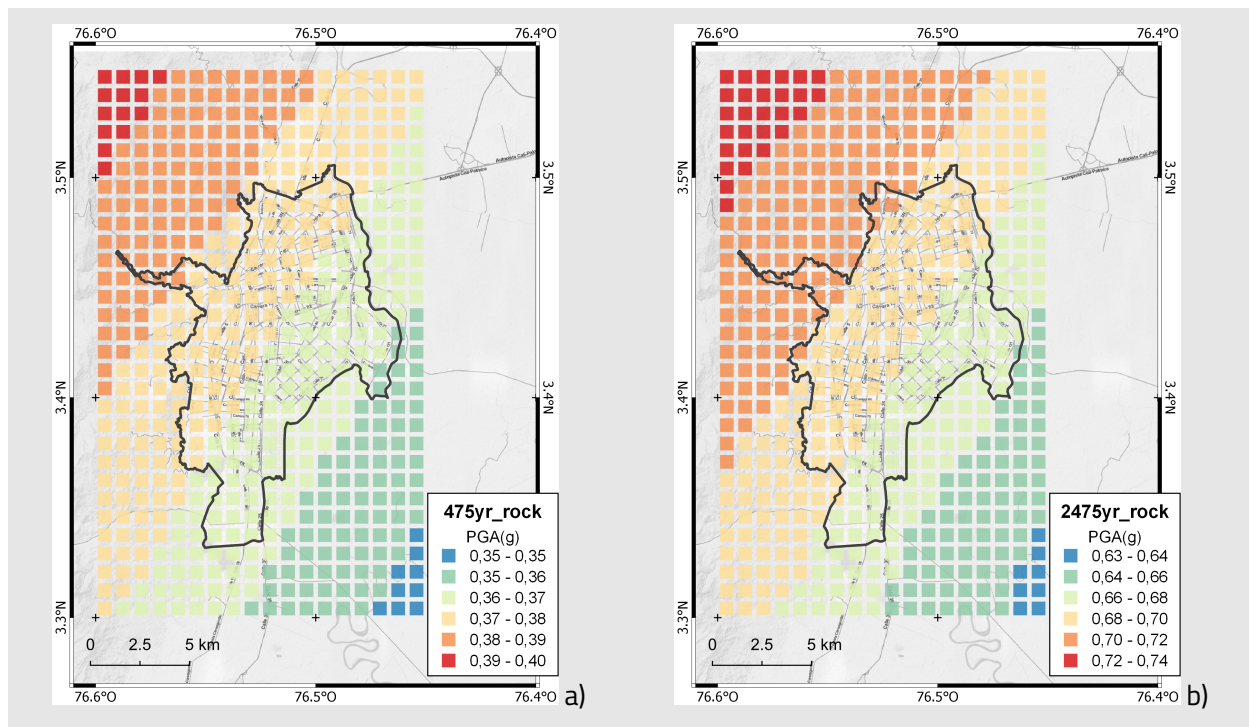


Figure 9. Mean PGA map for Santiago de Cali city (rock conditions): a) with 10% and b) 2% PoE in 50 years.

We also performed the disaggregation analysis for a site in the city (76.523°W and 3.443°N) as a combination of a) magnitude, distance and epsilon, b) longitude, latitude and tectonic region and c) longitude, latitude, and magnitude. The analysis was focused on PGA with a 10% PoE in 50 years on rock conditions ($V_{s30} = 800$ m/s), and seismic sources within 200 km were considered. Figure 10a shows results

for a combination of magnitude-distance-epsilon binned by 0.5 Mw and 10 km. As in Arcila et al. (2020), the largest contribution comes from sources at $\sim 80 - 100$ km distance with $M_w \sim 7.0 - 7.5$. This cluster can be associated to subduction intraslab sources taking into account the hazard contribution results presented in Figure 10b, where a combination of latitude-longitude and tectonic region is considered. The second cluster in Figure 10a is close to or within the city (~ 5 km) with $M_w \sim 6.0 - 7.0$. In this case, the hazard is dominated by active shallow crustal faulting (see Figure 10b).

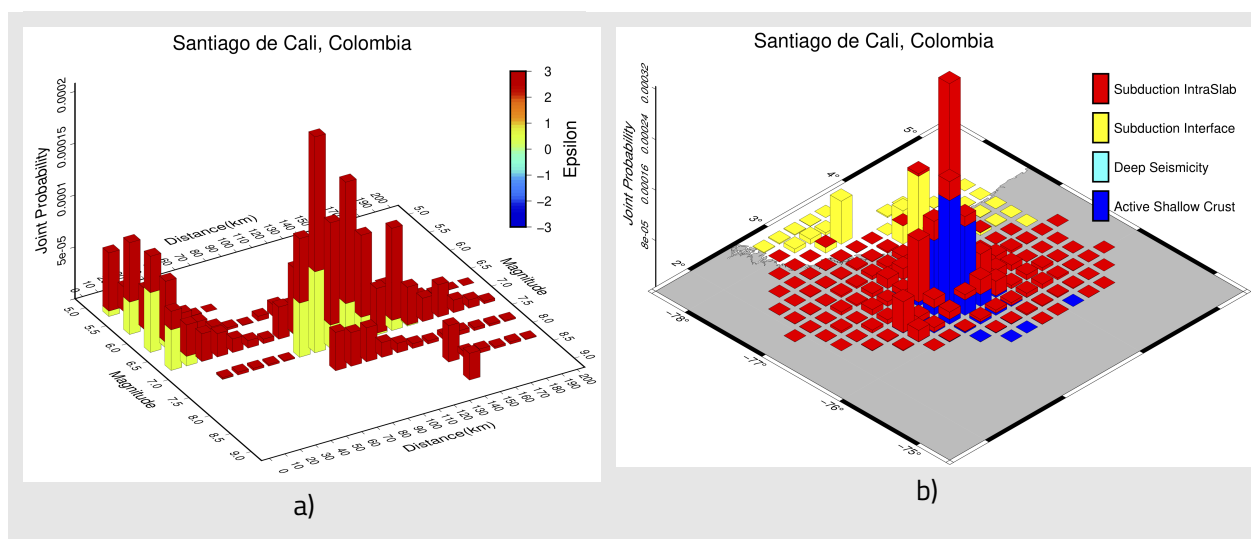


Figure 10. Disaggregation plots for mean PGA with 10% PoE in 50 years for Santiago de Cali city (rock conditions): a) magnitude - distance -epsilon (number of standard deviations from the mean of a GMPE), and b) latitude-longitude-tectonic region.

2.3 Seismic hazard results on Soil

The dramatic effects of ground motions amplified by local soil is well-known to the earthquake engineering community. Then, evaluation of the potential ground shaking generated for the contribution of surficial geology is a crucial component in PSHA, particularly for local and detailed seismic hazard studies. Unfortunately, information regarding seismic site-conditions is not always available and several methodologies had been developed to derive this information using proxies.

The most used methodology is the one proposed by Allen and Wald (2007), in which a global model of seismic site-conditions in terms of average shear-velocity down to 30 m (V_{s30}) was derived based on topography and topography slope. This methodology (model) is routinely used in the creation of near real-time shake-maps following occurrence of larger earthquakes. This methodology has well-known limitations (i.e. sites where slope is a relatively poor predictor), but overall, for a simplified analysis, this approach provides a robust first-order estimation of the seismic site-condition in regions where this information is poor.

o not available. Currently, the USGS provides a web service (<https://earthquake.usgs.gov/data/vs30/>) to deliver three styles of site condition mapping: a) topography (slope) based, b) a mosaic of slope and geologically based and c) a customised version using Vs30-slope coefficients provided by the user for a specific region.

Here, we used the global Vs30 USGS model to generate site-models covering the Santiago de Cali city and to be used in seismic hazard computations. In the case of Colombia, the slope and mosaic proxy models are available (Figure 11). The mosaic model (Figure 11b) predicts larger Vs30 values than the slope model for this specific case. Since to create the mosaic model local data were used (i.e. geomorphology, geology, site measurements), it was the model used to compute hazard estimation on soil conditions.

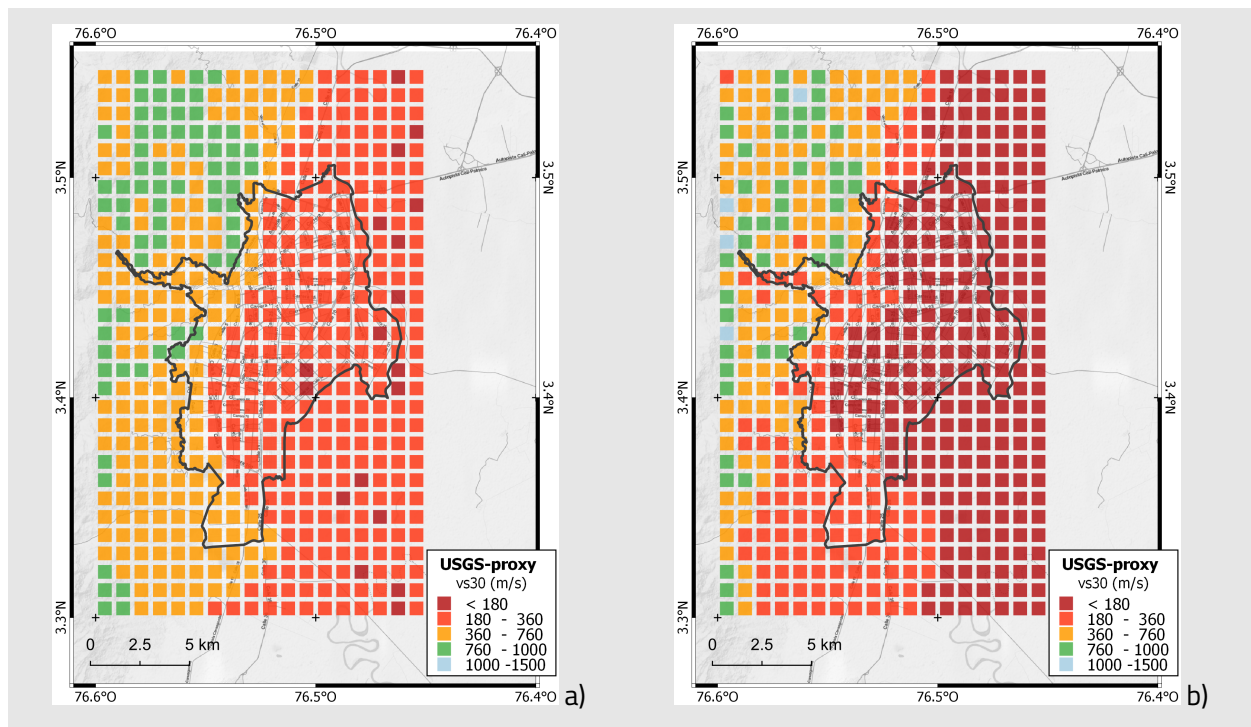


Figure 11. Estimated site condition for Cali city derived from: a) USGS slope proxy and b) USGS mosaic proxy.

2.3.1 Results using V_s30 from USGS

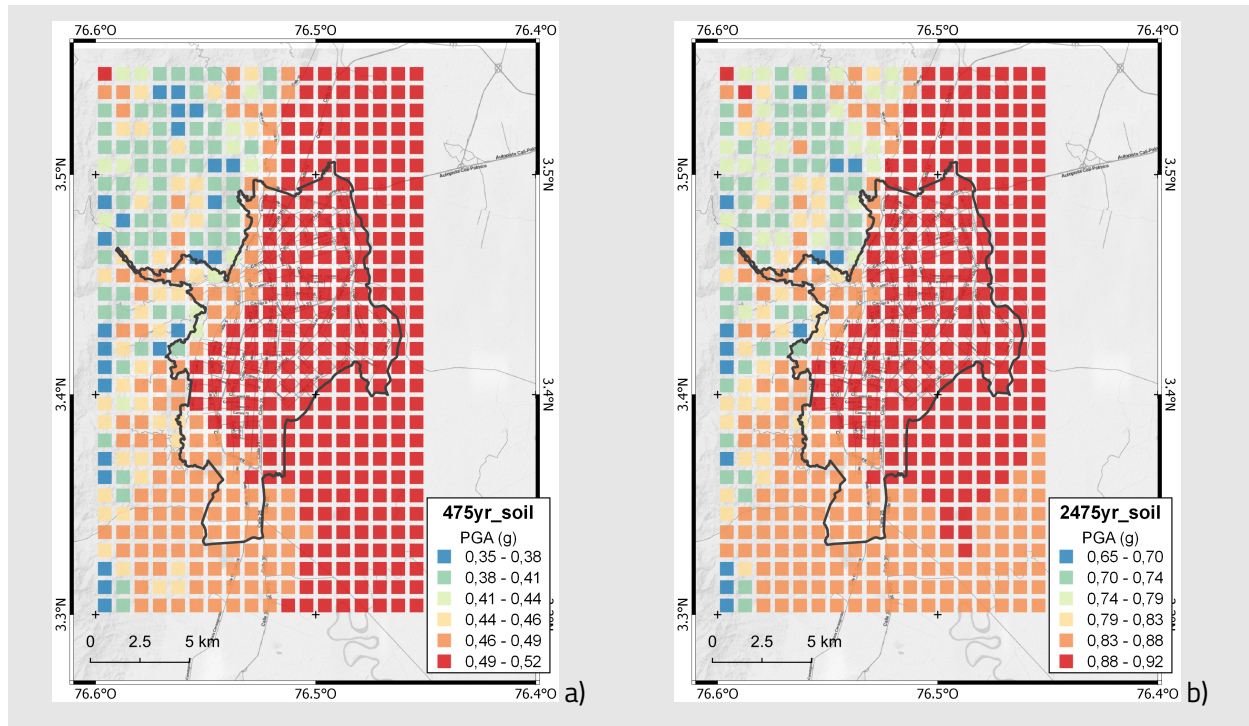


Figure 12. Mean PGA map for Santiago de Cali city (soil conditions): a) with 10% and b) 2% PoE in 50 years.

In Figure 12 the PGA maps for soil conditions using the USGS mosaic proxy are presented. In both cases, the highest PGA values are located at the east side of the city, reaching 0.52g and 0.92g for 10% and 2% PoE in 50 years, respectively. The hazard values decrease for the southern and western part of the city, with values mostly ranging 0.44 – 0.46g for 10% PoE in 50 years and 0.79 – 0.83g for 2% PoE in 50 years. The lowest values are located in the Cordillera (< 0.38g and 0.70g for 10% and 2% PoE in 50 years, respectively).

2.4 Comparison of results and discussion

To better demonstrate the influence of soil amplification on the hazard results for Santiago de Cali, a comparison between the mean hazard values for PGA (10% PoE in 50 years) and SA at 1.0 seconds (2% PoE in 50 years) based on a fixed V_s30 value (800 m/s) and hazard results considering spatially variable V_s30 computed using USGS V_s30 models was performed. The ratio (soil/rock) of the hazard values for the two spectral ordinates considered are presented in Figure 13. The values computed can be considered as the “amount” of hazard (ground shaking) being amplified by the near-surface soils.

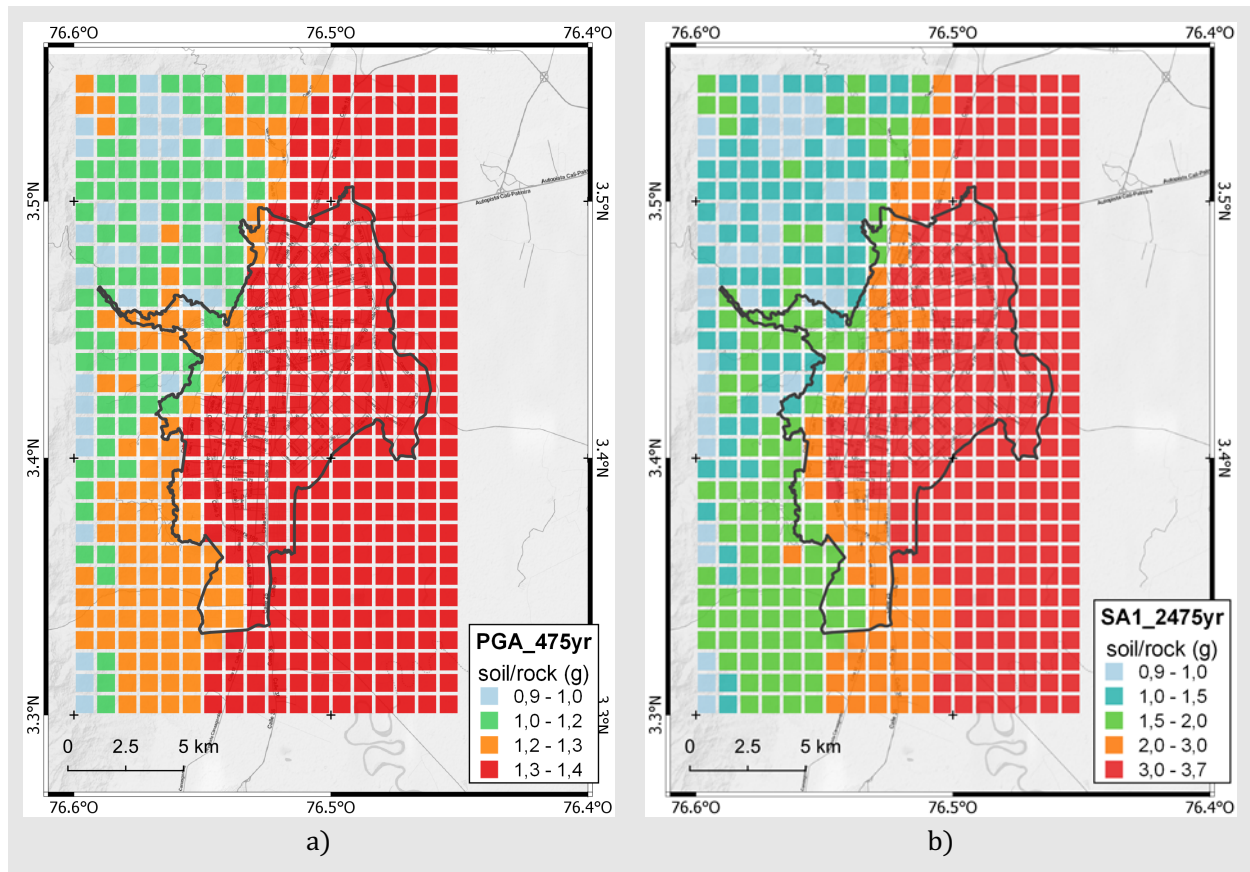


Figure 13. Soil amplification maps for Santiago de Cali city: a) PGA with 10% PoE in 50 years, b) SA at 1.0s for 2% PoE in 50 years. The amplification was computed as the ratio between the hazard values obtained using variable Vs30 (USGS mosaic model) and those for rock ($V_{s30} = 800$ m/s).

From the maps, it is evident that in an extensive part of the city there is a significant amount of site amplification. Site-conditions increase the shaking potential by 25% for PGA (10% PoE in 50 years), and by more than 65% for SA at 1.0 seconds (2% PoE in 50 years). The ratio is $\sim 1.3g$ for PGA and reached 3.0 – 3.7 g for almost the same area for SA at 1.0 seconds. This is due to the poor consolidated quaternary deposits covering the city represented by lowest Vs30 values (< 180 m/s) on the USGS mosaic model. In the eastern part of the city the amplification decreases. This region located on the Western Cordillera terranes is mainly composed by oceanic rocks with Vs30 values close to 800 m/s.

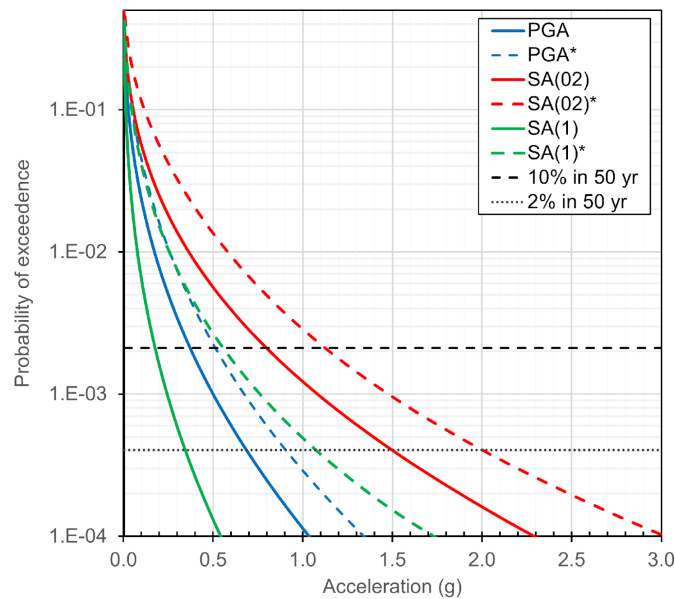


Figure 14. Hazard curves for Santiago de Cali city. The colored lines indicate acceleration for different structural periods (PGA, SA for 0.2 and 1.0 seconds) for rock condition ($V_{s30} = 800$ m/s) while dashed colored lines correspond to the same structural periods but referred to soil condition ($V_{s30} = 160$ m/s) The probability of exceedance (PoE) is for an investigation time of 1 year. Dashed and dotted black lines correspond to 2% and 10% PoE in 50 years respectively.

In Figure 14, the hazard curves computed for a site located at 76.523°W and 3.443°N are presented. The colored lines represent hazard computed for rock ($V_{s30} = 800$ m/s), while the dashed colored ones indicate hazard computed for a site with $V_{s30} = 160$ m/s, which could be considered representative for the most part of the city. The dashed and dotted horizontal black lines correspond to 2% and 10% PoE in 50 years, respectively. The curves confirmed that long period motions (SA at 1.0 seconds) are more influenced by variations in site conditions than ground shaking computed by PGA and SA at 0.2 seconds. There is a significant incrementation of SA at 1.0 second for 2% PoE in 50 years ($\sim 68\%$). The less influenced ordinate by site-conditions is PGA.

3 San Francisco de Quito, Ecuador

3.1 Reference National Seismic Hazard Model (NSHM)

The PSHA model proposed by Beauval et al. (2018) for Ecuador has been selected here as reference NSHM for Quito. This model benefits on a long-time scientific collaboration, relying on the most up-to-date information available in the country. Historical and instrumental seismicity were reviewed, as well as the active tectonic (Beauval et al., 2013; Alvarado et al. 2014). This favoured the definition of a new national seismic source model (Yepes et al., 2016) and hazard estimations.

The Beauval et al. (2018) seismic source model is composed by area sources (Figure 15a) enclosing the main active fault systems (Figure 15b) along the boundary between the NAB block and the SA plate. Two large background area sources were included to account for diffuse seismicity not associated with the faults considered. The catalogue was the main resource used to characterize the sources and three different

magnitude frequency distributions based on three diverse catalogues were used (see below). The fault model was developed using both, geologic and geodetic slip rate estimations, and three alternative models have been used (i.e. geodetic slip rate without aseismic deformation, geodetic slip rate with a 50% of aseismic deformation and geologic slip rate).

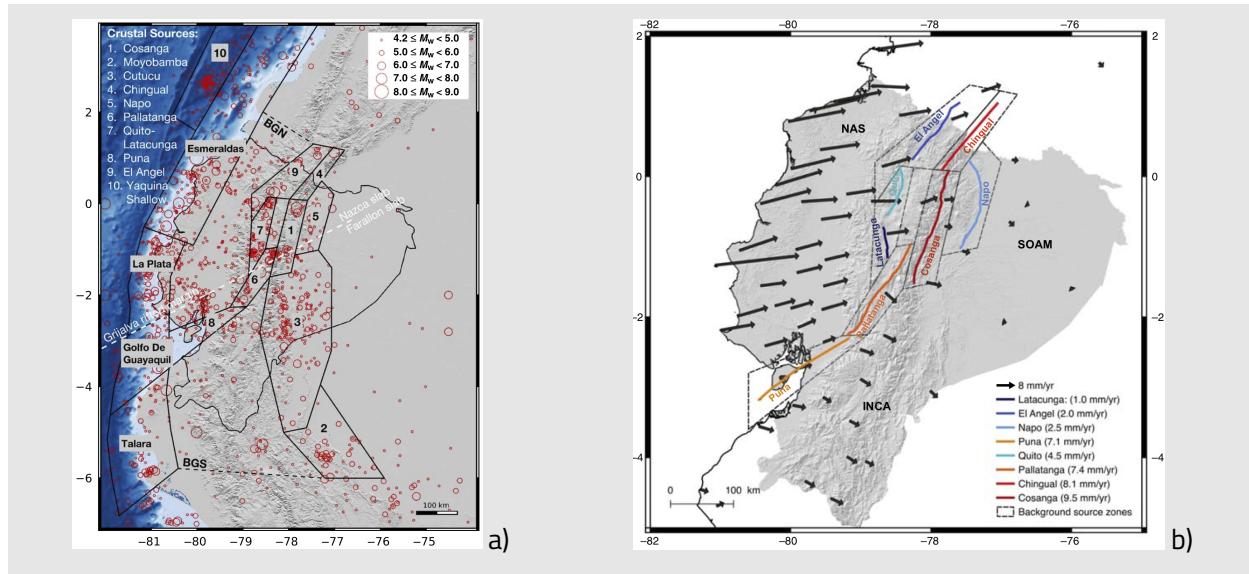


Figure 15. Beauval et al. (2018) PSHA study: a) crustal area sources (with numbers) and interface subduction sources (with names); and b) active shallow faults used to create the fault sources. Source: Beauval et al. (2018)

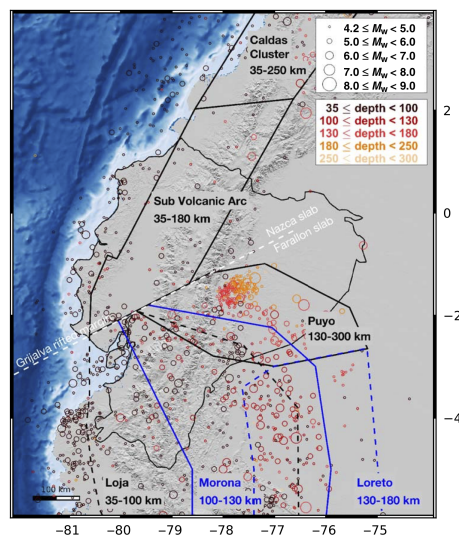


Figure 16. Beauval et al. (2018) PSHA study: a) intraslab sources. Source: Beauval et al. (2018)

The subduction interface sources are modelled as area sources too (Figure 15a). The segmentation of the subduction interface sources proposed by Yepes et al. (2016) was revised after the 2016 Pedernales M7.8 event. Then, the Esmeraldas source was extended 50 km farther to the south, consequently, the older Bahia source (called La Plata in Figure 15a) was reduced. In addition, the Talara segment was subdivided into two new segments (i.e. Golfo de Guayaquil and Talara).

The authors considered this new segmentation more consistent with the interseismic coupling information derived from GPS data and recorded history of large subduction earthquakes in Ecuador. Currently, the SSM contains four interface sources. The intraslab seismicity was modelled into volumes (Figure 16) defined at

increasing depths (events deeper than 35 km) to model the variations of the slab along dip direction. The Grijalva rift separates two different subducting plate domains. The most active Farallon domain contains four dipping volumes, while the Nazca domain contains two dipping volumes. In Yepes et al. (2016) a detailed description about the definition of the intraslab sources can be found.

For the characterization of area and volumes sources, three alternative earthquake catalogues were used. In addition to the Ecuador homogeneous catalogue, an ISC-based catalogue and a NEIC-based catalogue were considered. The uncertainties related to the process of building a homogeneous catalogue motivated this choice. Then, three alternative recurrence models were included in the logic tree (Figure 17).

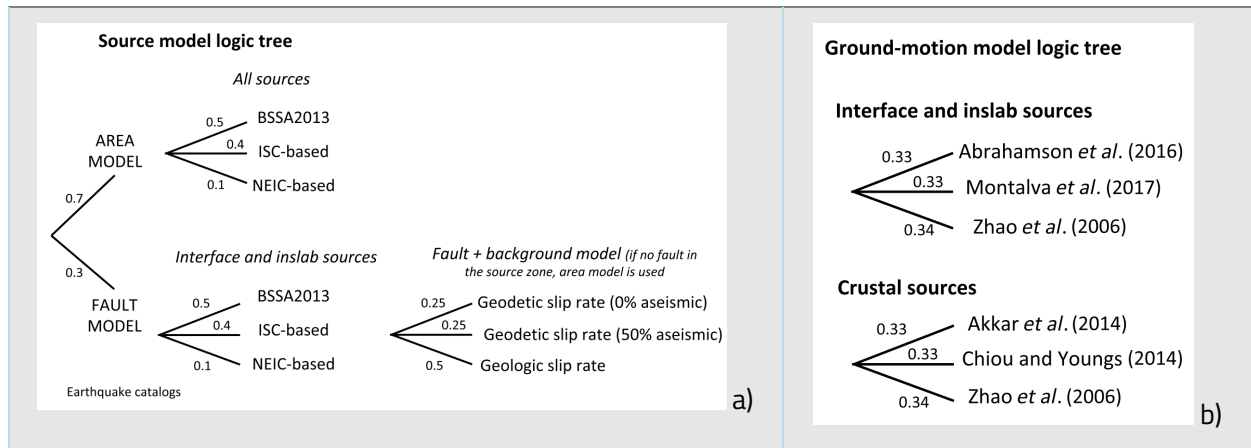


Figure 17. Beauval et al. (2018) PSHA study: a) source model logic tree, and b) ground motion logic tree. Source: Beauval et al. (2018)

The GMM was defined using models from literature. Three GMPEs for each tectonic environment were selected (i.e. interface, intraslab and shallow active sources). In the SSM logic tree, epistemic uncertainties related to two alternative models (area model and fault model) were considered. The use of three diverse recurrence rates leads to 12 alternative source models. The final logic tree (including the GMM logic tree) contains 324 different combinations.

The calculations were performed using the OpenQuake engine software (Pagani et al. 2014). The results published are referred to mean PGA and for a return period of 475 yrs, for a reference soil with $V_{s30} = 760$ m/s (see Figure 18). The highest PGA values are located along the coast in the north-western region (larger than 0.5 g). Higher values (larger than 0.4 g) are present inside the Cordillera. The lowest values are located in the north-eastern region. For Quito ~ 0.5 g is expected.

Unfortunately, the authors decided not to share with TREQ the full model, but only a simplified version of it. It is composed of shallow and subduction sources characterized using the ISC-based catalogue (see Figure YY3a) and active shallow fault sources developed considering geodetic slip-rates and assuming a 50% of aseismic slip. This version of the model is adequate for the purpose of this project and its expectative.

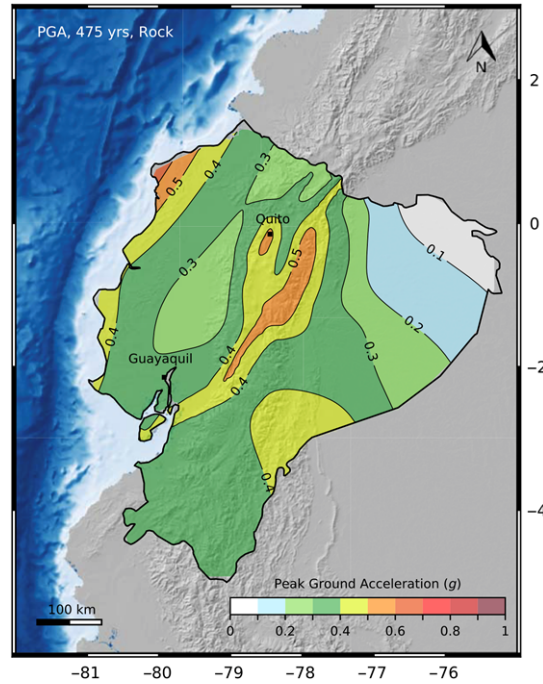


Figure 18. –. Mean PGA with 10% probability of exceedance in 50 years proposed by Beauval et al. (2018). Source: Beauval et al. (2018)

3.2 Seismic hazard results on Rock

3.2.1 Hazard results on reference bed rock

As for Cali, a reference bedrock with a $V_s = 800$ m/s has been considered a good compromise for hazard estimations on rock conditions. The calculations were performed for a grid covering the city (1 km spaced). Hazard maps, curves and UHSs were obtained for intensity measures PGA, SA at periods of 0.2 and 1.0 sec with 10% and 2% PoE in 50 years and for a reference bedrock equivalent to $V_{s30} = 800$ m/s.

In Figure 19 the PGA maps are presented. The highest PGA values reaching 0.56g and 1.11g for 10% and 2% PoE in 50 years, respectively are located in the central part of the city mostly influenced by the Quito fault source contribution. Medium hazard values are predicted for the western part of the city, which is affected by the subduction sources too, with values mostly ranging 0.50 – 0.45g for 10% PoE in 50 years and 1.1 – 1.0g for 2% PoE in 50 years. The lowest values are expected in the eastern region (~0.4g and 0.7g for 10% and 2% PoE in 50 years, respectively).

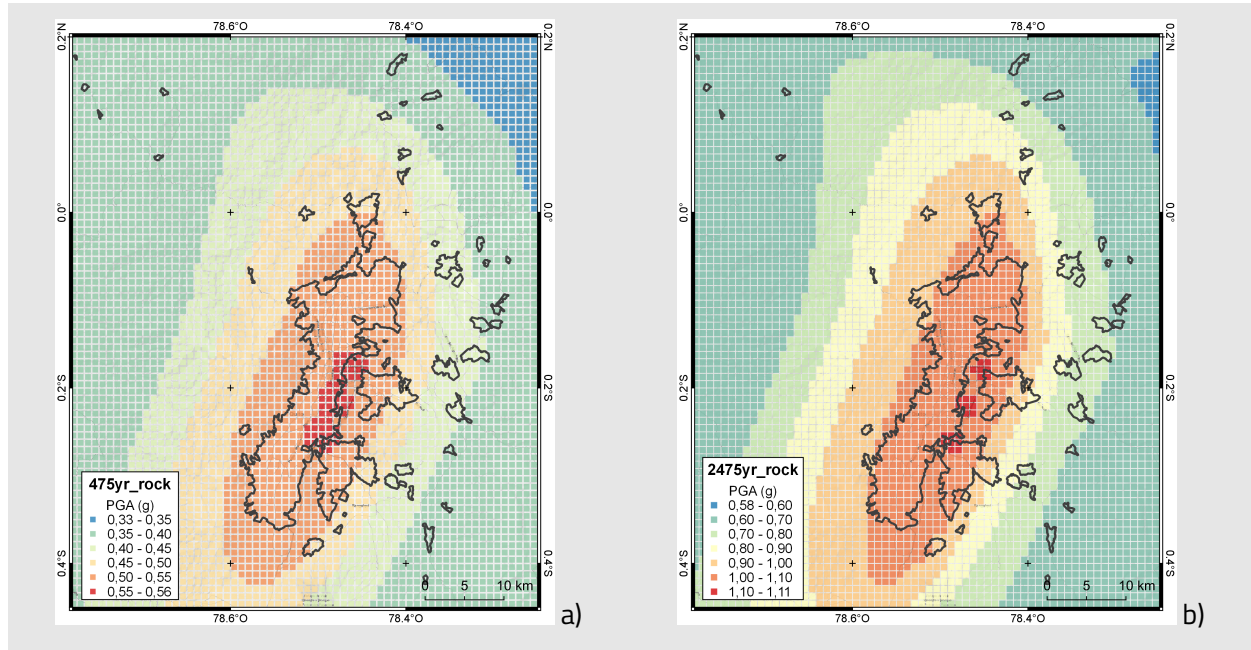


Figure 19. Mean PGA maps for Quito city (rock conditions): a) with 10% and b) 2% PoE in 50 years.

The disaggregation analysis for a site in the city (78.514°W and 0.221°S) was performed in the same manner that for Santiago de Cali, Colombia. Figure 20a shows results for a combination of magnitude-distance-epsilon binned by 0.5 Mw and 10 km. The hazard is dominated by active shallow sources (see Figure 20b) close to the city (~ 5 km) with $M_w \sim 6.5 - 7.5$, in particular by the (reverse) Quito fault system. Small contributions come from the subduction sources (at ~ 120 km) and probably, from other active shallow fault sources at ~ 50 km.

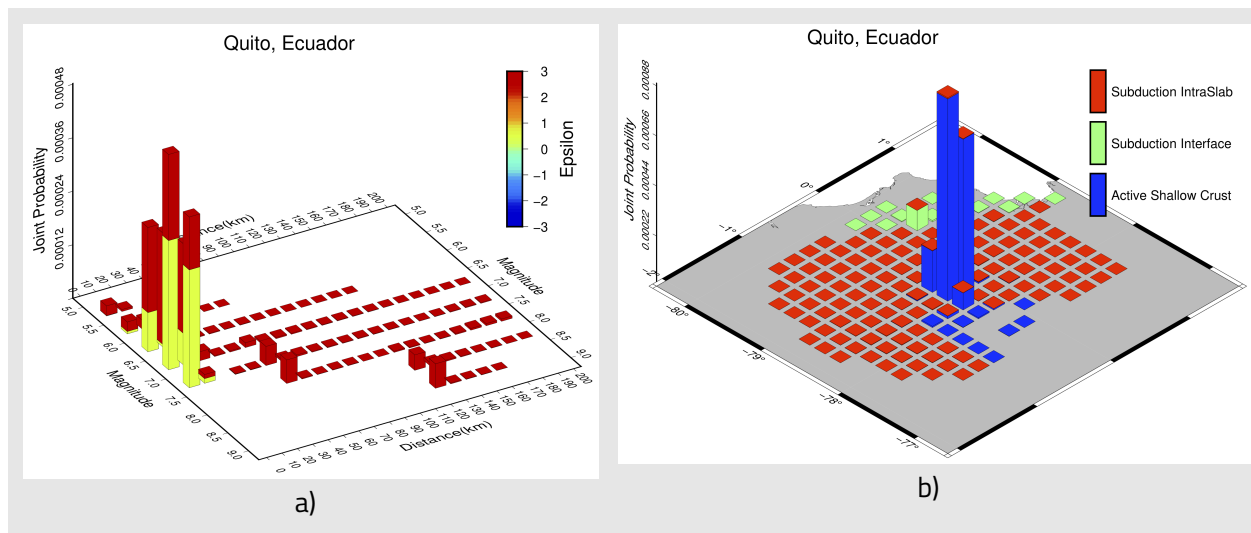


Figure 20. Disaggregation plots for mean PGA with 10% PoE in 50 years for Quito city (rock conditions): a) magnitude - distance - epsilon (number of standard deviations from the mean of a GMPE), and b) latitude-longitude-tectonic region.

3.3 Seismic hazard results on Soil

For Quito, the global Vs30 USGS model provides two proxy models (Figure 21), derived using SMRT topography and a mosaic of SMRT topography and other local data. The mosaic proxy model predicts larger Vs30 values than the slope proxy model. Here, we used the mosaic model to generate hazard results on soil conditions, since the mosaic model using local data probably provides a better resolution and a more reliable site model.

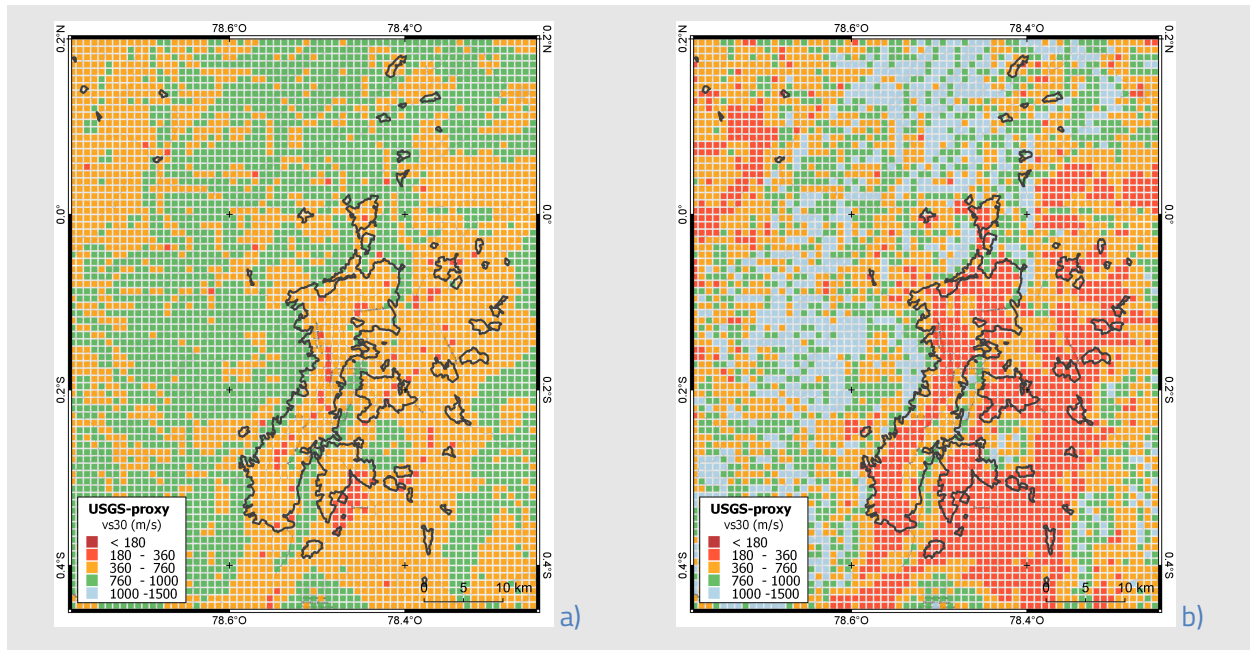


Figure 21. Estimated site condition for Quito city derived from: a) USGS slope proxy and b) USGS mosaic proxy.

3.3.1 Results using Vs30 from USGS

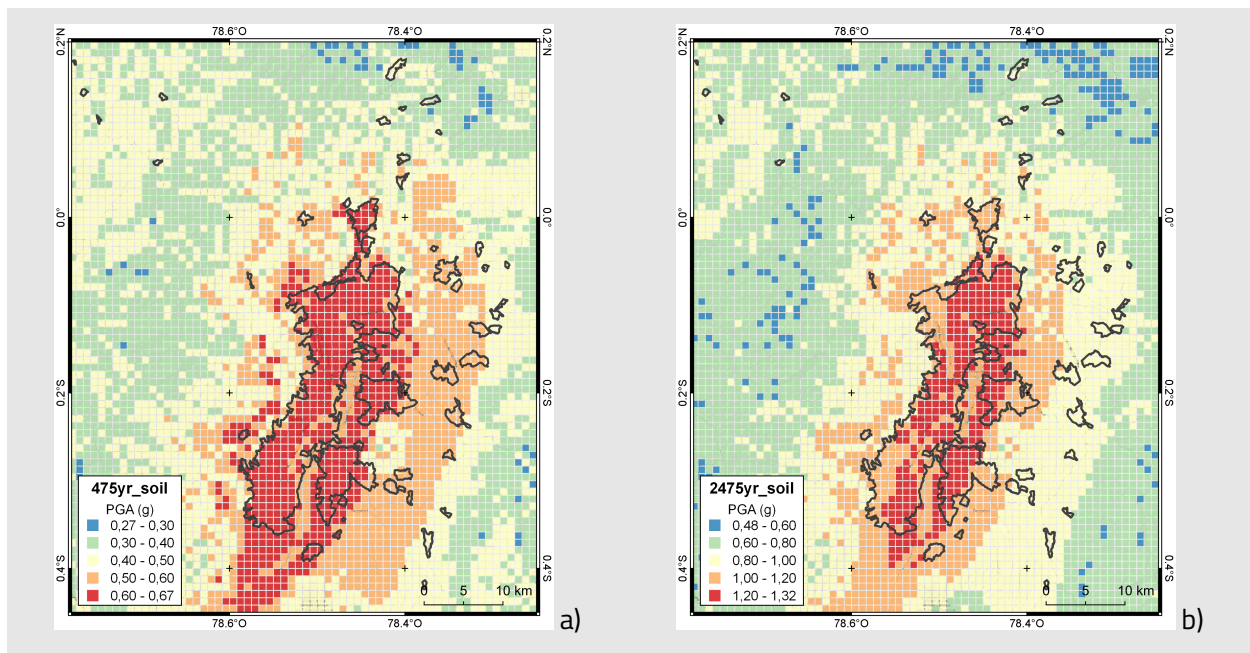


Figure 22. Mean PGA maps for Quito city (soil conditions): a) with 10% and b) 2% PoE in 50 years.

In Figure 22 the PGA maps for soil conditions using the USGS mosaic proxy are presented. The highest PGA values cover almost the whole city, reaching 0.67g and 1.32g for 10% and 2% PoE in 50 years, respectively. The hazard values decrease for the eastern part of the city, with values mostly ranging 0.50 – 0.60 g for 10% PoE in 50 years and 0.80 – 1.20g for 2% PoE in 50 years.

3.4 Comparison of results and discussion

As for Santiago de Cali city, in Figure 23, the ratio (soil/rock) for Quito city is presented. In this case, for PGA (10% PoE in 50 years) the site-conditions increase the shaking potential by a 15% (ratio = 1.2g) and by 45% for SA at 1.0 seconds and 2% PoE in 50 years (ratio ~1.5 – 2.0g). A small part of the city (i.e. San Rafael and Pifo) could be affected by larger amplifications for SA at 1.0 seconds and 2% PoE in 50 years (ratio > 2.0g). The amplifications are due to Quito city is built on Plio-Quaternary volcanoplastic basins, which contain volcanoclastic sediment sequences with V_{s30} values ranging, mostly, 250 – 400 m/s in the USGS mosaic model.

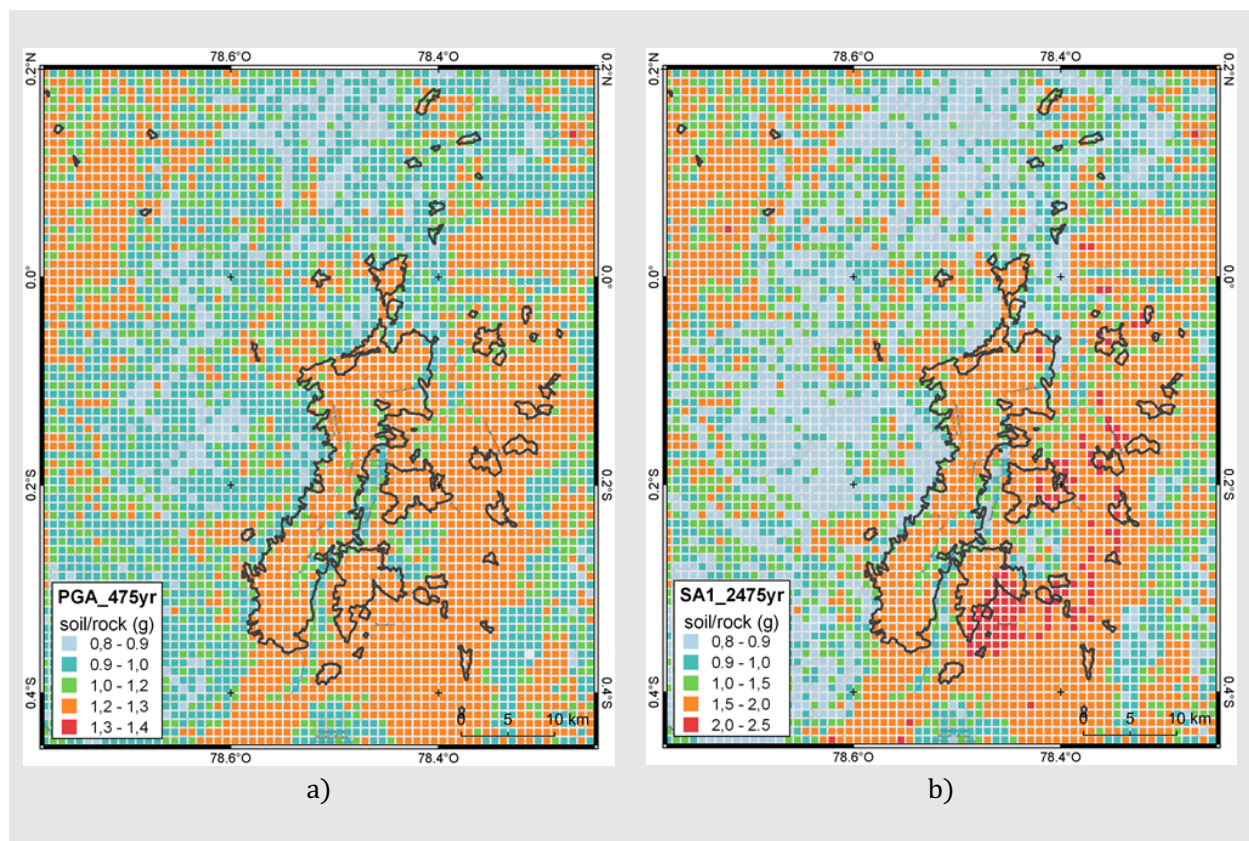


Figure 23. Soil amplification maps for Quito city: a) PGA with 10% PoE in 50 years, b) SA at 1.0s for 2% PoE in 50 years. The amplification was computed as the ratio between the hazard values obtained using variable V_{s30} (USGS mosaic model) and those for rock ($V_{s30} = 800$ m/s).

The hazard curves computed for a site located at 78.514°W and 0.221°S are presented in Figure 24. As for Cali, the colored lines represent hazard computed for rock ($V_{s30} = 800$ m/s), while the dashed colored ones indicate hazard computed for a site with $V_{s30} = 320$ m/s, which could be considered representative for the

most part of the city. The dashed and dotted horizontal black lines correspond to 2% and 10% PoE in 50 years respectively.

From the curves it is evident that long period motions (SA at 1.0 seconds) are more influenced by variations in site conditions than ground shaking computed by PGA and SA at 0.2 seconds. The amplification for SA at 1.0 seconds is significant, ~32% for 10% PoE in 50 years and larger for 2% PoE in 50 years (~48%). For SA at 0.2 seconds the amplification is lesser (15% for both, 10% and 2% PoE in 50 years) and PGA is the less influenced ordinate by site conditions.

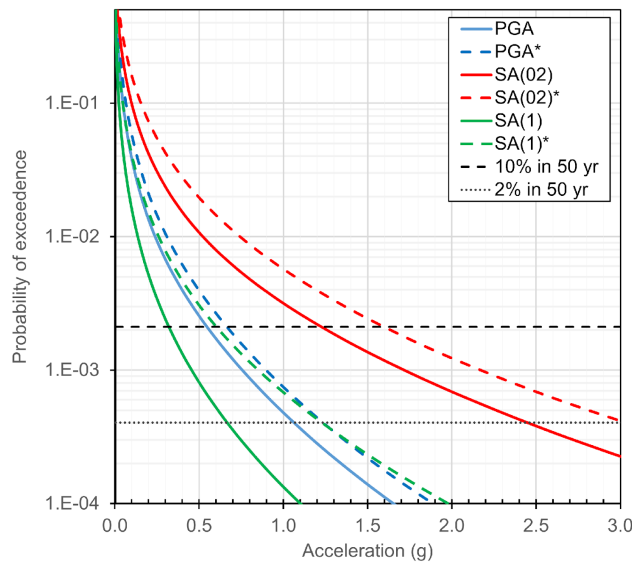


Figure 24. Hazard curves for Quito city. The colored lines indicate acceleration for different structural periods (PGA, SA for 0.2 and 1.0 seconds) for rock condition ($V_{s30} = 800$ m/s) while dashed colored lines correspond to the same structural periods but referred to soil condition ($V_{s30} = 320$ m/s) The probability of exceedence (PoE) is for an investigation time of 1 year. Dashed and dotted black lines correspond to 2% and 10% PoE in 50 years, respectively.

4 Santiago de los Caballeros, The Dominican Republic

4.1 Reference NSHM

In the framework of the TREQ project, we worked with local experts from the National Geological Survey (SGN) and the Autonomous University of Santo Domingo (UASD) at compiling, reviewing, and preparing basic data sets needed to build a reference NSHM for the Dominican Republic; the model is referred to herein as DOM21.

The seismic source characterization (SSC) for DOM21 has the following major characteristics:

- **Active shallow crustal seismicity** is modelled by fault sources modelled using ruptures that can span one or multiple faults, and distributed seismicity modelled as gridded smoothed seismicity. This part of the SSC includes epistemic uncertainty in the smoothing approach, maximum magnitude via scaling relationship, on-to-off fault seismicity ratio, and productivity rate of some major fault sources. The poorly constrained North Hispaniola and Los Muertos trench interfaces are included in this part of the model.

- **Subduction interface seismicity** associated with the Puerto Rico Trench is modelled by OpenQuake Engine complex faults using two end-member magnitude frequency distributions
- **Subduction intraslab seismicity** in the North Hispaniola and Puerto Rico Trenches modelled by OpenQuake Engine non-parametric ruptures constrained to the subducting slab volume with epistemic uncertainty in the rates accounted for by (1) uniform distribution versus (2) distribution based on past occurrences.

The ground motion characterization (GMC) selected of the work done in the framework of the CCARA project since no specific ground motion recording and GMPEs were available for this study. The PSHA model is described in detail in TREQ D2.2.2.

4.2 Seismic hazard results on Rock

Figure 25 shows the hazard in terms of mean PGA on rock with a 10% and 2% POE in 50 years for Santiago de los Caballeros. In general, the hazard increases from southwest to northeast across the city, ranging from ~0.3 – 0.7g for the higher POE and ~0.7 – 1.4 g for the lower POE. The seismic hazard results on rock, including seismic hazard disaggregation for Santiago de los Caballeros, are described in much greater detail in TREQ D2.2.2.

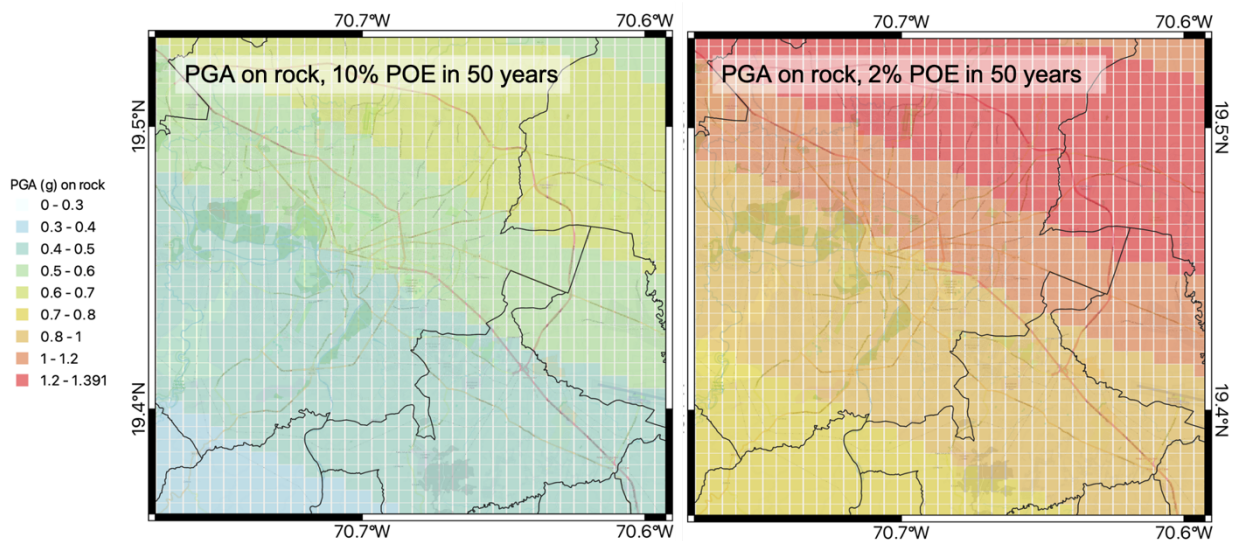


Figure 25. PGA on rock in the vicinity of Santiago de los Caballeros with (left) 10% and (right) 2% POE in 50 years.

4.3 Seismic hazard results on Soil

For Santiago de los Caballeros, the global Vs30 USGS model provides the proxy Vs30 values derived using SMRT topography (Figure 26); these Vs30 values were used to generate hazard results on soil conditions.

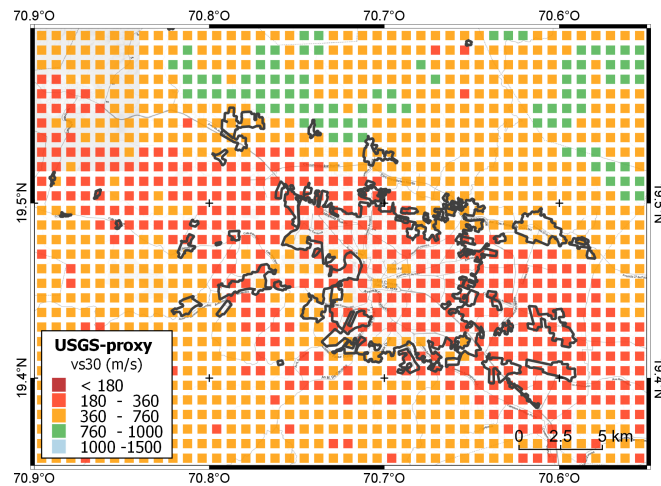


Figure 26. Estimated site condition for Santiago de los Caballeros city derived from USGS slope proxy.

4.3.1 Results using V_{s30} from USGS

Figure 27 shows the PGA maps computed for soil conditions using the USGS V_{s30} proxy in Figure 26. In both cases, the highest PGA values are located at the north-eastern side of the city, reaching 0.79g and 1.6g for 10% and 2% PoE in 50 years, respectively. Across the city, there is a bit more scatter in the hazard, and the band of peak hazard is more confined than for the hazard on rock.

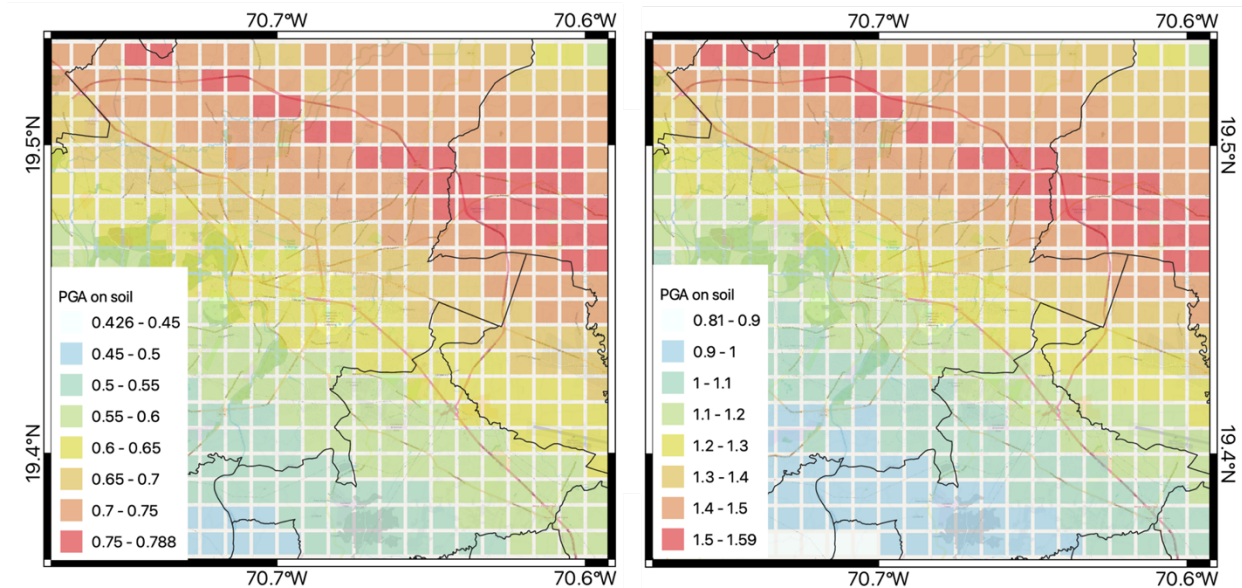


Figure 27. Mean PGA map for Santiago de los Caballeros city (soil conditions): a) with 10% and b) 2% PoE in 50 years.

5 Conclusions

This report describes the geographic distribution of hazard computed by the three pilot cities considered by the TREQ project. The selected national seismic hazard models (NSHM) have been used to compute seismic hazard on reference bedrock, as well as on soil condition using a simplified approach, which accounts for

expected ground shaking on soil using the time-averaged velocity of shear waves in the uppermost 30 m (V_{s30}).

The hazard calculations were performed for rock and soils conditions on a grid covering the cities and for 10% and 2% PoE in 50 years. The results were computed for several structural periods (peak ground acceleration and spectral acceleration at 0.2, 0.5, 1.0 and 2.0 seconds) on rock and soil conditions, which were compared to have a first approximation of the potential expected ground shaking due to locally soil conditions.

The rock condition was fixed to a $V_{s30} = 800$ m/s for the three cities, but site condition on soil hazard computation depends on V_{s30} global model proposed by the USGS (Allen and Wald, 2007). For Santiago the Cali and Quito cities, the "mosaic" version of this model was used. Since for Santiago de los Caballeros the "mosaic" version is not available, the "slope - based" version was considered.

From maps and curves created to understand the influence (and variability) of site-conditions on hazard results, it was evident that long-periods motions (SA at 1.0 s) are more influenced by variations in site conditions than short periods (PGA and/or SA at 0.2 s). Therefore, low period hazard maps (and curves) must be considered as a future descriptor of the overall hazard for the three cities. In addition, the disaggregation results obtained must be considered to create future scenarios for these cities.

6 References

- Abrahamson, N. A., Gregor, N., and Addo, K. (2016). BC Hydro Ground Motion Prediction Equations for Subduction Earthquakes. *Earthquake Spectra*, 32(1), 23-44. doi:10.1193/051712eqs188mr
- Abrahamson, N. A., W. J. Silva, and R. Kamai (2014). Summary of the ASK14 ground motion relation for active crustal regions, *Earthq. Spectra* 30, 1025–1055.
- AIS (2009), Estudio General de Amenaza Sísmica de Colombia (2009). Asociación Colombiana de Ingeniería Sísmica – AIS. Comité AIS-300, Bogotá, 227 pp
- Akkar S., M. A. Sandikkaya, and J. J. Bommer (2014). Empirical Ground-Motion Models for Point- and Extended-Source Crustal Earthquake Scenarios in Europe and the Middle East, *Bulletin of Earthquake Engineering* (2014), 12(1): 359 - 387
- Allen, T.I., and Wald, D.J. (2007). Topographic slope as a proxy for global seismic site conditions (VS30) and amplification around the globe: U.S. Geological Survey Open-File Report 2007-1357, 69 p
- Alvarado A., Audin L., Nocquet J. M., Lagreulet S., et al., (2014). Active tectonics in Quito, Ecuador, assessed by geomorphological studies, GPS data, and crustal seismicity. *Tectonics*. 33(2): 67-83. doi: 10.1002/2012TC003224.
- Arcila, M. García, J., Montejo, J., Eraso, J., Valcarcel, J., Mora, M., Viganò, D., Pagani, M. y Díaz, F. (2020). Modelo nacional de amenaza sísmica para Colombia. Bogotá: Servicio Geológico Colombiano y Fundación Global Earthquake Model. <https://doi.org/10.32685/9789585279469>
- Arcila, M., García-Mayordomo, J., y López, M.C (2017, septiembre) Modelo de zonas sismogénicas para la evaluación de la amenaza sísmica de Colombia. Ponencia presentada en el XVI Congreso Colombiano de Geología. Santa Marta, Colombia, 1540-1543
- Atkinson Gail M. and David M. Boore (2006). Earthquake Ground-Motion Prediction Equations for Eastern North America; *Bulletin of the Seismological Society of America*, Volume 96, No. 6, pages 2181-2205
- Atkinson G. M. and D. M. Boore (2003). Empirical ground-motion relations for subduction zone earthquakes and their application to Cascadia and other regions. *Bulletin of the Seismological Society of America*, 93(4):1703-1729, 2003.
- Bazzurro, Paolo, and Cornell, C. Allin (2004). Nonlinear soil-site effects in probabilistic seismic hazard analysis: *Bulletin of the Seismological Society of America*, v. 94, p. 2110–2123.
- Beauval C., J. Marinière, H. Yepes, L. Audin, J.-M. Nocquet, A. Alvarado, S. Baize, J. Aguilar, J.-C. Singaicho, H. Jomard (2018). A New Seismic Hazard Model for Ecuador. *Bulletin of the Seismological Society of America*; 108 (3A): 1443–1464. doi: <https://doi.org/10.1785/0120170259>
- Beauval, C., Yepes, H., Palacios, P., Segovia, M., Alvarado, A., Font, y Vaca, S. (2013). An Earthquake Catalog for Seismic Hazard Assessment in Ecuador. *Bulletin of the Seismological Society of America*, 103(2a), 773-786.
- Bernal, G. (2014), Metodología para la modelación, cálculo y calibración de parámetros de la amenaza sísmica para la evaluación probabilista del riesgo. (Tesis Doctoral). Universidad Politécnica de Cataluña, Barcelona, España.
- Bertil D., Lemoine A., Winter T., Belvaux M. (2010) – Microzonificación sísmica de Santiago – Republica Dominicana. Amenaza regional. Informe final. BRGM/RC-59107-FR, 100 p., 36 fig., 12 tablas, 2 anexos.

- Cauzzi, C., Faccioli, E., Vanini, M. y Bianchini, A. (2014). Updated predictive equations for broadband (0.01-10 s) horizontal response spectra and peak ground motions, based on a global dataset of digital acceleration records. *Bulletin of Earthquake Engineering*, 13, 1587-1612. <http://dx.doi.org/10.1007/s10518-014-9685-y>
- Chiou, B. S.-J. and R. R. Youngs (2014). Update of the Chiou and Youngs NGA model for the average horizontal component of peak ground motion and response spectra. In: *Earthquake Spectra* 30.3, pages 1117–1153.
- Cornell, C. (1968). Engineering seismic risk analysis, *Bull. Seismol. Soc. Am.* 58, 1568–1606.
- Frankel, A. (1995). Mapping seismic hazard in the central and eastern United States. *Seismological Research Letters*, 66(4), 8-21.
- Gerstenberger, M.C., Marzocchi, W., Allen, T. & Pagani, M., Adams, J., Danciu, L., Field, E.H., Fujiwara, H., Luco, Nicolas, Ma, K.-F., Meletti, C., Petersen, M.D. (2020). Probabilistic Seismic Hazard Analysis at Regional and National Scale: State of the Art and Future Challenges. *Reviews of Geophysics*. 10.1029/2019RG000653.
- Hayes, Gavin P., David J. Wald, and Rebecca L. Johnson. (2012). Slab1. 0: A three-dimensional model of global subduction zone geometries. *Journal of Geophysical Research: Solid Earth* 117.B1 (2012).
- Hayes, G. P., Moore, G. L., Portner, D. E., Hearne, M., Flamme, H., Furtney, M., & Smoczyk, G. M. (2018). Slab2, a comprehensive subduction zone geometry model. *Science*, 362(6410), 58-61.
- Idriss, I. (2014). An NGA-West2 empirical model for estimating the horizontal spectral values generated by shallow crustal earthquakes. *Earthquake Spectra*, 30 (3), 1155-1177. <http://dx.doi.org/10.1193/072813EQS219M>.
- INGEOMINAS-DAGMA. (2005). Estudio de microzonificación sísmica de Santiago de Cali. Bogotá. Ministerio de Minas y Energía
- Leonard, M. (2014). Self-consistent earthquake fault-scaling relations: Update and extension to stable continental strike-slip faults. *Bulletin of the Seismological Society of America*, 104 (6), 2953- 2965. <http://dx.doi.org/10.1785/0120140087>.
- Leonard, M. (2010). Earthquake fault scaling: Relating rupture length, width, average displacement, and moment release, *Bull. Seismol. Soc. Am.* 100, no. 5A, 1971–1988.
- Llorente Isidro, M., Belvaux M., Bernardez E., Bertil D., Fernandez-Merodo J., Lain-Huerta L., Lopera-Caballero E., Muños-Tapia S. and Roullé A. (2017). Geología para el estudio de microzonación sísmica en Santiago de los Caballeros, República Dominicana. *Boletín Geológico y Minero*, 128 (3): 715-736, ISSN: 0366-0176, DOI: 10.21701/bolgeomin.128.3.010
- McGuire, R. K. (2004), *Seismic hazard and risk analysis*, Earthquake Engineering Research Institute, Oakland, California.
- Montalva, G. A., Bastias, N., and Rodriguez-Marek, A. (2017). Ground-Motion Prediction Equation for the Chilean Subduction Zone, *Bulletin of the Seismological Society of America*, 107(2), 901-911
- NSR-10. Reglamento Colombiano de la Construcción Sismorresistente, Cámara Colombiana de la Construcción. Decreto 926 del 19 de marzo de 2010. <http://www.camacol.co> (último acceso enero de 2015).
- Pagani, M., Johnson, K., Garcia-Pelaez, J. (2020). Modelling subduction sources for probabilistic seismic hazard analysis. Geological Society, London, Special Publications. SP501-2019. 10.1144/SP501-2019-120.

- Pagani M, Monelli D, Weatherill G, Danciu L, Crowley H, Silva V, Henshaw P, Butler L, Nastasi M, Panzeri L, Simionato M, Vigano D (2014). OpenQuake Engine: An Open Hazard (and Risk) Software for the Global Earthquake Model. *Seismol Res Lett* 85:692–702
- Roullé, A.; Vanoudheusden, E.; Belvaux, M.; Auclair S. (2011): Microzonificación sísmica de Santiago – Republica Dominicana. Amenaza sísmica local. Informe BRGM/ RC-59685-FR, 103 p.
- Salgado-Gálvez, M.A., Bernal, G.A., y Cardona, O.D (2016). Evaluación probabilista de la amenaza sísmica de Colombia con fines de actualización de la Norma Colombiana de Diseño de Puentes CCP-14” *Revista Internacional de Métodos Numéricos para Cálculo y Diseño en Ingeniería*, 32(4), 230-239.
- Styron, R. and García-Pelaez, J. and Pagani, M. (2019). CCAF-DB: The Caribbean and Central American Active Fault Database, *Nat. Hazards Earth Syst. Sci. Discuss.*, 1-42, <https://doi.org/10.5194/nhess-2019-46>, in review, 2019.
- Yepes, H., L. Audin, A. Alvarado, C. Beauval, J. Aguilar, Y. Font, and F. Cotton (2016). \, *Tectonics* 35, doi: 10.1002/2015TC003941
- Zhao, J. X., Zhang, J., Asano, A., Ohno, Y., Oouchi, T., Takahashi, T., Ogawa, H., Irikura, K., Thio, H. K., Somerville, P. G., Fukushima, Y., and Fukushima, Y. (2006). Attenuation relations of strong ground motion in Japan using site classification based on predominant period. *Bulletin of the Seismological Society of America*, 96(3), 898–913.